Opinion

Proposed Guidelines for Hypertriglyceridemia in Japan with Non-HDL Cholesterol as the Second Target

Hitoshi Shimano, Hidenori Arai, Mariko Harada-Shiba, Hirotsugu Ueshima, Takao Ohta, Shizuya Yamashita, Takanari Gotoda, Yutaka Kiyohara, Toshio Hayashi, Junji Kobayashi, Kazuaki Shimamoto, Hideaki Bujo, Shun Ishibashi, Koji Shirai, Shinichi Oikawa, Yasushi Saito, and Nobuhiro Yamada

The Research Committee for Primary Hyperlipidemia, Research on Measures for Intractable Diseases by the Ministry for Health, Labor, and Welfare in Japan.

The Japan Atherosclerosis Society (JAS) guidelines for the prevention of atherosclerotic diseases, proposing management for LDL cholesterol as the primary target, have successfully contributed to the prevention of cardiovascular events; however, recently, the impact of hypertriglyceridemia as an additional cardiovascular risk has become understood, especially in light of the rise in obesity, metabolic syndrome, and diabetes in the Japanese population. Rather than waiting to obtain conclusive domestic data confirming that hypertriglyceridemia is a cardiovascular risk factor and that its management is efficacious, we propose guidelines for hypertriglyceridemia using non-HDL cholesterol as a second target.

J Atheroscler Thromb, 2008; 15:116-121.

Key words; Hyperlipidemia, Dyslipidemia, Triglycerides, HDL cholesterol, LDL cholesterol

Introduction

Many prospective epidemiological studies have indicated a positive relationship between serum triglyceride (TG) levels and the incidence of coronary heart disease (CHD)[1, 2]. TG-rich lipoproteins such as remnant lipoproteins and small dense LDL particles are increased in hypertriglyceridemia and have been established to be atherogenic by numerous clinical and experimental studies[3-6]; however, classification of the plasma TG level as an independent risk factor for atherosclerosis has been controversial. This is partly because plasma TG levels are inversely intercorrelated by other well-established risk factors, such as low HDL cholesterol. To date, large scale trials for intervention targeting plasma TGs with TG reducing agents such as fibrates have not reached definitive conclusions about their effectiveness on primary endpoints, although fibrates have some impact on both primary and secondary prevention in small scale studies[7-9].

The precise estimation of plasma TGs as a cardiovascular risk is confounded by other risk factors, such as obesity, diabetes, hypertension and smoking. In addition, a cluster of metabolic risk factors, such as visceral obesity and insulin resistance with hypertriglyceridemia, referred to as metabolic syndrome, indicates that plasma TG concentrations are tightly linked to other strong risk factors for CHD. Thus, patients with elevated TGs are at increased risk for CHD, although greater risk cannot be independently explained by TGs. Meanwhile, recent meta-analyses suggested that plasma TGs could be an independent factor for CHD[1, 2]. Supportively, many experimental studies indicated that triglyceride-rich lipoproteins as well as LDL are atherogenic. Taken together, these data suggest that hypertriglyceridemia should be regarded as a semi-independent risk factor and should be included as a clinical target for the prevention of CHD. Considering the increasing prevalence of obesity, metabolic syndrome, and diabetes in this country, guidelines specialized for patients with hypertriglyceridemia need to be immediately established. In this study, we propose new guidelines for Japanese patients with hypertriglyceridemia

Address for correspondence: Hitoshi Shimano, Department of Internal Medicine (Endocrinology and Metabolism) Graduate School of Comprehensive Human Sciences University of Tsukuba, 1-1-1Tennodai, Tsukuba Ibaraki 305-8575, Japan.
E-mail: shimano-tky@umin.ac.jp
Received: November 22, 2007
Accepted for publication: February 2, 2008

Table 1. Plasma lipid profile of severe and mild type Ⅱb hyperlipidemic patients sub-grouped by non-HDL cholesterol level

Male	severe type Ⅱb non-HDLc >190 mg/dL	mild type Ⅱb non-HDLc <190 mg/dL	p
n	51	54	
Total Cholesterol	270±41.8	234±40.3	0.001
Triglycerides	347±286	236±110	0.031
HDL Cholesterol	42.4±8.0	54.9±15.2	0.000
LDL Cholesterol	159±51.6	135±38.1	0.029
non-HDL Cholesterol	228±41.6	182±39.1	0.000

Female	severe type Ⅱb non-HDLc >180 mg/dL	mild type Ⅱb non-HDLc <180 mg/dL	p
n	52	48	
Total Cholesterol	265±29.6	231±20.2	0.000
Triglycerides	242±120	218±56	0.1
HDL Cholesterol	47.3±14.1	63.2±19.5	0.000
LDL Cholesterol	175±40.4	125±17.9	0.000
non-HDL Cholesterol	224±30.2	168±14.9	0.000

Subjects were patients who visited the outpatient clinic of the Endocrinology and Metabolism Unit of Tsukuba University Hospital on a regular basis (monthly or bimonthly) as described in Materials and Methods. Data are the means±SD (mg/dL).

using non-HDL as a secondary target after the goal for LDL cholesterol as the primary target is achieved.

Materials and Methods

A total of 1,124 patients in Tsukuba University hospital in 2006 were consecutively included in the study (**Table 1**). Patients with severe illness were excluded. Plasma total cholesterol (TC), LDL-C, TG, HDL-C, glucose and HbA1c in either the fasted or fed state were determined enzymatically with the Hitachi 7070. Plasma HDL-C concentration was measured by a direct method using polyethylene-glycoso-pretreated enzymes. We calculated LDL-C concentration with Friedewald's formula (TC-TG/5-HDL-C) when TG was less than 400 mg/dL. Plasma non-HDL-C concentration was calculated as TC − HDL-C. One hundred and five male and 100 female patients were diagnosed with Type Ⅱb hyperlipidemia (TC>220 mg/dL and TG>150 mg/dL). They were subcategorized into two groups according to their non-HDL cholesterol level (**Table 1**).

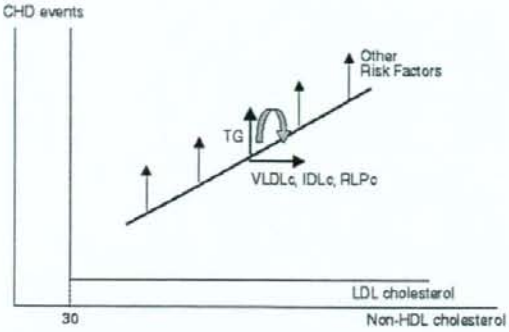

Fig. 1. Rationale for usage of non-HDL cholesterol: impact of TG and other risk factors on correlation between LDL-cholesterol CHD event.

nonHDL cholesterol = Total cholesterol − HDL cholesterol = VLDL cholesterol + IDL cholesterol (remnant lipoprotein cholesterol) + LDL cholesterol (Friedewald formula).
VLDL cholesterol + IDL cholesterol (RLP cholesterol) = TG/5
The risk of hypertriglyceridemia is approximated to VLDL, IDL, and RLP cholesterol estimated as TG/5, and incorporated into non-HDLC. The difference between non-HDL cholesterol and LDL cholesterol on X-axis was set up at 30 mg/dL based upon the data from Fig. 2.

Results and Discussion

Advantage of Non-HDL Cholesterol as a Marker for Hypertriglyceridemia

LDL cholesterol has been established as the most potent predictor of CHD and is currently the primary target for treatment and prevention. Other risk factors, including TG, diabetes, obesity, and metabolic syndrome, do not directly elevate plasma LDL cholesterol, but could enhance the risk of LDL cholesterol by shifting up the curve, as depicted in **Fig. 1**. To evaluate and manage the risk of hypertriglyceridemia, the TG level must be interpolated into the risk of plasma cholesterol. In patients with high TGs, most VLDL cholesterol resides in the smaller (remnant) VLDL fraction. Cholesterol of remnant lipoproteins (VLDL and IDL), which is concomitantly increased by elevation of plasma TG is an appropriate surrogate marker of hypertriglyceridemia. TG-rich remnant lipoproteins have been established as atherogenic lipoproteins[4, 5]. Thus, RLPc, a commercially available laboratory test for remnant lipoprotein cholesterol, could be a suitable marker for the atherogenicity of hypertriglyceridemia; however, this test is expensive and is not practical for use as a routine parameter. In contrast, non-HDL cholesterol, defined as total cholesterol − HDL cholesterol, is easily calculated, and represents the sum-

mation of VLDL/IDL (remnant) cholesterol and LDL cholesterol. It reflects the risks for all apoB-containing lipoproteins and could be an excellent marker for atherogenic lipoproteins. Plasma TG itself is not an appropriate marker for CHD risk due to its internal and dietary variability. In contrast, non-HDL cholesterol is not affected by dietary states and has much less daily variability than TG.

Predictive Power of Non-HDL Cholesterol

Non-HDL cholesterol reflects the risks of both hypertrigyceridemia and LDL-cholesterol[10, 11]. Several studies have indicated that non-HDL cholesterol is better than LDL cholesterol in its predictive power of cardiovascular diseases, indicating that VLDL cholesterol could contribute to CVD[12]. Non-HDL cholesterol is also a useful marker in a variety of subpopulations: men, the elderly, and patients with high-risk diseases such as diabetes and end-stage renal disease[13-16]. Our current clinical data from patients with type IIb hyperlipidemia also support the usefulness of non-HDL cholesterol (**Table 1**). In our outpatient clinic, 70% of patients had diabetes and roughly 10% were type IIb hyperlipidemia (cholesterol > 220 mg/dL and TG > 150 mg/dL). These type IIb hyperlipidemic patients were equally divided into two sub-groups: severe (non-HDL cholesterol levels ≥ 190 mg/dL for male patients and 180 mg/dL for female patients) and mild < 190 mg/dL for male patients and 180 mg/dL for female patients. When the severe and mild IIb groups were compared, total, LDL, HDL cholesterol, and TG levels were significantly different among these two groups for both genders, except for serum triglyceride in females (**Table 1**). These data indicate that non-HDL cholesterol is an excellent marker representing all the components of dyslipidemia. The usefulness of non-HDL cholesterol rather than low-density lipoprotein cholesterol as a tool for lipoprotein cholesterol screening and assessment of risk and therapy has been already recognized in the USA[17, 18]. Another candidate marker for both remnant and LDL cholesterol is plasma apoB level[19]. ApoB is a direct marker for the particle number of apoB-containing lipoproteins and reflects risks of both remnants and LDL. Non-HDL cholesterol is highly correlated with apoB, and should replace this specialized and expensive laboratory test despite some reports indicating that apoB is better than non-HDL cholesterol for the predictive power of CHD[15, 20].

However, according to the Friedewald formula, the TG risk in non-HDL cholesterol represents only one fifth of TG levels as remnant cholesterol, and thus, the contribution of the risk is relatively weak compared to that of LDL cholesterol. Our previous data indicated that the correlation of non-HDL cholesterol to LDL cholesterol was much stronger than that to the TG level (**Fig. 2**)[21]. It should be noted that non-HDL cholesterol is not a specific marker for hypertriglyceridemia. Rather, non-HDL cholesterol should be regarded as a general single marker for both hypercholesterolemia and/or hypertriglyceridemia.

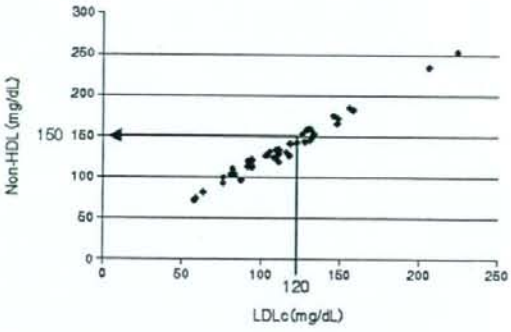

Fig. 2. Distribution of non-HDL cholesterol vs. calculated LDL cholesterol in normolipidemic patients.

Non-HDL cholesterol and LDL cholesterol calculated from Friedewald formula were highly correlated. Subjects were from the outpatient clinic of Tsukuba University Hospital[21].

Proposed Guidelines for Hypertriglyceridemia

Based upon these considerations, we propose guidelines for hypertriglyceridemia in Japanese patients using non-HDL cholesterol as a secondary target, as shown in **Table 2**. This is an extended version of the 2007 edition of the Japan Atherosclerosis Society (JAS) guidelines for the prevention of atherosclerotic diseases in which LDL cholesterol is the primary marker and target. It is essentially similar to the AHA-ATPIII guidelines for hyperTG in USA[22]. ATPIII recommends using non-HDL cholesterol as a secondary target when plasma TG is greater than 200 mg/dL because VLDL cholesterol is not significantly accumulated if TG is less than 200 mg/dL[23]. We do not have enough clinical data for Japanese on the relationship between TG and VLDL cholesterol to provide the appropriate TG level where the use of a non-HDL marker should be considered. Currently, we recommend using non-HDL for patients with hypertriglyceridemia (TG > than 150 mg/dL). Even for patients with hypertriglyceridemia, the primary target is still LDL cholesterol. In the 2007 JAS guidelines, goals of LDL for the secondary prevention group and the primary prevention group with category I, II, and III are 100, 120, 140, and 160 mg/

Table 2. Proposed Japanese Guidelines for Hypertriglyceridemia

Treatment	Categories	Coronary Risk Factors other than LCL-C	Goal for plasma lipids (mg/dL) Primary LDL-C	Secondary nonHDL-C	HDL-C
Primary Prevention Improving lifestyle as the first line, followed by medication	I (Low Risk Group)	0	<160	<190	≥ 40
	II (Intermediate)	1～2	<140	<170	
	III (High)	≥ 3	<120	<150	
Secondary Prevention Improving lifestyle & medication	Past History of CHD		<100	<130	

Goals for control depend upon categories of LDL cholesterol and non-HDL cholesterol. The primary target in hypertriglyceridemia is LDL-cholesterol. If the goal for LDL-cholesterol in the Japanese Guidelines for Atherosclerosis 2007 is already achieved, nonHDL-C is the secondary target. For the patients with TG>500 mg/dL, potential genetic disorders and the prevention of acute pancreatitis should be considered. Coronary risk factors other than LDL-cholesterol include low HDL cholesterol, aging, diabetes, hypertension, smoking, past history of CHD, and obesity (visceral obesity).

dL, respectively. Goals for non-HDL cholesterol in each group are those for LDL cholesterol plus 30 mg/dL. This is based upon our outpatient clinic data that non-HDL cholesterol was 30 mg/dL higher than LDL cholesterol (**Fig. 2**)[21]. ATPIII also recommends using LDL cholesterol goal + 30 mg/dL[24]. This also corresponds to the calculated VLDL cholesterol of the cut-off point of normal TGs (150/5 mg/dL). This goal is arbitrarily set and could be modified in the future, especially when the relative atherogenicity of remnants and LDL cholesterol are more precisely determined. In the case of TGs of greater than 500 mg/dL, the risk of pancreatitis should be carefully considered as a potential acute complication.

Treatment of Hypertriglyceridemia Based upon Non-HDL Cholesterol Level

Treatment of patients with hypertriglyceridemia for primary prevention should be initiated with lifestyle modifications, especially reducing weight and increasing physical activity. Lifestyles exacerbating hypertrigylyceridemia, such as overweight, obesity, physical inactivity, cigarette smoking, excess alcohol intake, and very high carbohydrate diets, need to be improved. Other disorders and drugs that cause secondary hypertriglyceridemia, including diabetes, chronic renal filure, nephrotic syndrome, and steroid therapy, should also be treated first. In the event that lifestyle modification for at least three months is not effective to achieve the goal of non-HDL cholesterol, medication should be considered. Currently, due to lack of evidence to fully justify the use of fibrates for high TGs prior to statins, it is recommended to use a statin as the first line choice for high non-HDL cholesterol. If statin therapy is already used to control LDL cholesterol, management of non-HDL should be targeted by increasing the dose of the statin or switching to a stronger form. This is based upon the notion that remnant lipoproteins, as well as LDL, are taken up through LDL receptors that are up-regulated by statins. In the case of type III hyperlipidemia, or if high non-HDL cholesterol is much more prominent than LDL cholesterol because of hypertriglyceridemia, fibrates could be considered as they specifically reduce plasma TGs and are effective against type III hyperlipidemia. However, LDL cholesterol should be carefully monitored since fibrates occasionally raise LDL cholesterol following a decrease in TGs (VLDL cholesterol). In case the goal for LDL cholesterol is not attainable, the addition of cholestimide and/or ezetimibe to statin could be considered, whereas EPA could be considered for hypertriglyceridemia. A positive result from a recent large scale Japanese study using both EPA and pravastatin to estimate the prevention of atherosclerotic events, justifies superimposing EPA on statin therapy, although the contribution of the plasma TG-lowering effect of EPA to the prevention of cardiovascular events is not yet determined[25]. The complexity of the choice of medication for high non-HDL cholesterol is currently inevitable because no agents specifically decrease non-HDL cholesterol. Drug information strongly warns against the use of both statins and fibrates because of increasing the risk of the life-threatening side effect of rhabdomyolysis. Joint use is justified only when the benefit exceeds the risk, which requires expertise in this field; however, considering the very few reports of rhabdomyolysis as a severe side effect in recent post-market studies in Japan, carefully prescribing both agents for high-risk patients such as those with type IIb hyperlipidemia could be re-considered. Joint use might be restricted in the elderly or renal compromised patients. In addition, monitoring mus-

cle symptoms and plasma creatine phosphokinase is necessary in patients prescribed either statins or fibrates.

Conclusions and Future Prospect of the Guidelines

Non-HDL cholesterol containing both LDL cholesterol and remnant cholesterol, is an excellent predictor of atherosclerotic risk, and should be a treatment target. Non-HDL cholesterol is simple, convenient, and free from dietary variations. These advantages are crucial for nation-wide use of the guidelines and health check activity. This simple measurement could also make it possible to re-evaluate previous clinical studies using this parameter to offer a good chance of estimating the usefulness and importance of this marker in a large meta-analytical scale.

In the current study, we propose that LDL cholesterol is the primary target and non-HDL cholesterol should be the secondary target for elevated TG. Considering that non-HDL and LDL cholesterol are partially redundant, non-HDL could replace LDL as the primary target and as a general marker for both elevated cholesterol and TG. As **Table 1** shows, non-HDL cholesterol could be used as a general and convenient lipid marker for type IIb hyperlipidemia.

This proposal still faces the recent problem of selecting lipid markers for the initial assessment for dyslipidemia. The recent GL focus has been on LDL cholesterol rather than TC, while LDL cholesterol has a problem the lower reliability for direct measurement. In addition, a considerable portion of hypertriglyceridemia is not applicable to this equation. For subjects with hypertriglyceridemia, application of this new GL eventually requires all TC, TG, HDL, and LDL cholesterol measurements to assess both LDL and non-HDL cholesterol. Currently, however, the Japanese medical system covers only three out of four lipid measurements as healthcare services provided by health insurance. Further Japanese clinical studies and careful evaluation of the data, as well as technical improvements of reliable LDL cholesterol measurements, are required to determine the most efficient protocol to select lipid measurements as the initial assessment of dyslipidemia to prevent CVD in Japan. Furthermore, guidelines for HDL cholesterol should also be established, although the relative importance and positioning of non-HDL and HDL is yet to be determined.

Acknowledgements

This work is supported by Health and Labor Sciences Research Grants from the Ministry for Health, Labor, and Welfare in Japan. We thank Prof. Y. Nakamura, Drs Y. Miyashita, K. Okada, H. Yagyu, T. Imamura, and S. Saito for helpful discussion, and Drs K. Takekoshi, H. Toyoshima, H. Suzuki, A. Takahashi, K. Saito, S. Kawabe, M. Ishikawa, H. Iwasaki, Y. Iwasaki, and H. Danno for the study of patients with type IIb hyperlipidemia at Tsukuba University Hospital. We are also grateful to Dr. A.H. Hasty at Vanderbilt University for critical reading of the manuscript.

References

1) Assmann G, Schulte H, Funke H, and von Eckardstein A: The emergence of triglycerides as a significant independent risk factor in coronary artery disease. Eur Heart J, 1998; 19 Suppl M:M8-14
2) Austin MA, Hokanson JE, and Edwards KL: Hypertriglyceridemia as a cardiovascular risk factor. Am J Cardiol, 1998; 81:7B-12B
3) Krauss RM: Atherogenicity of triglyceride-rich lipoproteins. Am J Cardiol, 1998; 81:13B-17B
4) Grundy SM: Hypertriglyceridemia, atherogenic dyslipidemia, and the metabolic syndrome. Am J Cardiol, 1998; 81:18B-25B
5) Havel RJ: Role of triglyceride-rich lipoproteins in progression of atherosclerosis. Circulation, 1990; 81:694-696
6) Breslow JL: Mouse models of atherosclerosis. Science, 1996; 272:685-688
7) Elkeles RS, Diamond JR, Poulter C, Dhanjil S, Nicolaides AN, Mahmood S, Richmond W, Mather H, Sharp P, and Feher MD: Cardiovascular outcomes in type 2 diabetes. A double-blind placebo-controlled study of bezafibrate: the St. Mary's, Ealing, Northwick Park Diabetes Cardiovascular Disease Prevention (SENDCAP) Study. Diabetes Care, 1998; 21:641-648
8) Tenenbaum A, Motro M, Fisman EZ, Tanne D, Boyko V, and Behar S: Bezafibrate for the secondary prevention of myocardial infarction in patients with metabolic syndrome. Arch Intern Med, 2005; 165:1154-1160
9) Keech A, Simes RJ, Barter P, Best J, Scott R, Taskinen MR, Forder P, Pillai A, Davis T, Glasziou P, Drury P, Kesäniemi YA, Sullivan D, Hunt D, Colman P, d'Emden M, Whiting M, Ehnholm C, and Laakso M: Effects of long-term fenofibrate therapy on cardiovascular events in 9795 people with type 2 diabetes mellitus (the FIELD study): randomised controlled trial. Lancet, 2005; 366:1849-1861
10) Grundy SM: Non-high-density lipoprotein cholesterol level as potential risk predictor and therapy target. Arch Intern Med, 2001; 161:1379-1380
11) Packard CJ and Saito Y: Non-HDL cholesterol as a measure of atherosclerotic risk. J Atheroscler Thromb, 2004; 11:6-14
12) Liu J, Sempos CT, Donahue RP, Dorn J, Trevisan M, and Grundy SM: Non-high-density lipoprotein and very-low-density lipoprotein cholesterol and their risk predictive values in coronary heart disease. Am J Cardiol, 2006; 98:1363-1368
13) Pischon T, Girman CJ, Sacks FM, Rifai N, Stampfer MJ, and Rimm EB: Non-high-density lipoprotein cholesterol

and apolipoprotein B in the prediction of coronary heart disease in men. Circulation, 2005; 112:3375-3383
14) Kawamoto R, Oka Y, Tomita H, and Kodama A: Non-HDL cholesterol as a predictor of carotid atherosclerosis in the elderly. J Atheroscler Thromb, 2005; 12:143-148
15) Jiang R, Schulze MB, Li T, Rifai N, Stampfer MJ, Rimm EB, and Hu FB: Non-HDL cholesterol and apolipoprotein B predict cardiovascular disease events among men with type 2 diabetes. Diabetes Care, 2004; 27:1991-1997
16) Nishizawa Y, Shoji T, Kakiya R, Tsujimoto Y, Tabata T, Ishimura E, Nakatani T, Miki T, and Inaba M: Non-high-density lipoprotein cholesterol (non-HDL-C) as a predictor of cardiovascular mortality in patients with end-stage renal disease. Kidney Int Suppl, 2003; 84:S117-120
17) Frost PH and Havel RJ: Rationale for use of non-high-density lipoprotein cholesterol rather than low-density lipoprotein cholesterol as a tool for lipoprotein cholesterol screening and assessment of risk and therapy. Am J Cardiol, 1998; 81:26B-31B
18) Cui Y, Blumenthal RS, Flaws JA, Whiteman MK, Langenberg P, Bachorik PS, and Bush TL: Non-high-density lipoprotein cholesterol level as a predictor of cardiovascular disease mortality. Arch Intern Med, 2001; 161:1413-1419
19) Vega GL and Grundy SM: Does measurement of apolipoprotein B have a place in cholesterol management? Arteriosclerosis, 1990; 10:668-671
20) Simon A, Chironi G, Gariepy J, Del Pino M, and Levenson J: Differences between markers of atherogenic lipoproteins in predicting high cardiovascular risk and subclinical atherosclerosis in asymptomatic men. Atherosclerosis, 2005; 179:339-344
21) Sugimoto K, Isobe K, Kawakami Y, and Yamada N: The relationship between non-HDL cholesterol and other lipid parameters in Japanese subjects. J Atheroscler Thromb, 2005; 12:107-110
22) Third Report of the National Cholesterol Education Program (NCEP) Expert Panel on Detection, Evaluation, and Treatment of High Blood Cholesterol in Adults (Adult Treatment Panel III) final report. Circulation, 2002; 106:3143-3421
23) Goldstein JL, Schrott HG, Hazzard WR, Bierman EL, and Motulsky AG: Hyperlipidemia in coronary heart disease. II. Genetic analysis of lipid levels in 176 families and delineation of a new inherited disorder, combined hyperlipidemia. J Clin Invest, 1973; 52:1544-1568
24) Heiss G, Tamir I, Davis CE, Tyroler HA, Rifkand BM, Schonfeld G, Jacobs D, and Frantz ID Jr.: Lipoprotein-cholesterol distributions in selected North American populations: the lipid research clinics program prevalence study. Circulation, 1980; 61:302-315
25) Yokoyama M, Origasa H, Matsuzaki M, Matsuzawa Y, Saito Y, Ishikawa Y, Oikawa S, Sasaki J, Hishida H, Itakura H, Kita T, Kitabatake A, Nakaya N, Sakata T, Shimada K, and Shirato K: Effects of eicosapentaenoic acid on major coronary events in hypercholesterolaemic patients (JELIS): a randomised open-label, blinded endpoint analysis. Lancet, 2007; 369:1090-1098

ORIGINAL ARTICLE

Palmitate Impairs and Eicosapentaenoate Restores Insulin Secretion Through Regulation of SREBP-1c in Pancreatic Islets

Toyonori Kato,[1] Hitoshi Shimano,[1,2] Takashi Yamamoto,[1] Mayumi Ishikawa,[1] Shin Kumadaki,[1] Takashi Matsuzaka,[1,2] Yoshimi Nakagawa,[1,2] Naoya Yahagi,[2] Masanori Nakakuki,[1] Alyssa H. Hasty,[3] Yoshinori Takeuchi,[1] Kazuto Kobayashi,[1] Akimitsu Takahashi,[1] Shigeru Yatoh,[1] Hiroaki Suzuki,[1] Hirohito Sone,[1] and Nobuhiro Yamada[1]

OBJECTIVE—Chronic exposure to fatty acids causes β-cell failure, often referred to as lipotoxicity. We investigated its mechanisms, focusing on contribution of SREBP-1c, a key transcription factor for lipogenesis.

RESEARCH DESIGN AND METHODS—We studied in vitro and in vivo effects of saturated and polyunsaturated acids on insulin secretion, insulin signaling, and expression of genes involved in β-cell functions. Pancreatic islets isolated from C57BL/6 control and SREBP-1–null mice and adenoviral gene delivery or knockdown systems of related genes were used.

RESULTS—Incubation of C57BL/6 islets with palmitate caused inhibition of both glucose- and potassium-stimulated insulin secretion, but addition of eicosapentaenoate (EPA) restored both inhibitions. Concomitantly, palmitate activated and EPA abolished both mRNA and nuclear protein of SREBP-1c, accompanied by reciprocal changes of SREBP-1c target genes such as insulin receptor substrate-2 (IRS-2) and granuphilin. These palmitate-EPA effects on insulin secretion were abolished in SREBP-1–null islets. Suppression of IRS-2/Akt pathway could be a part of the downstream mechanism for the SREBP-1c–mediated insulin secretion defect because adenoviral constitutively active Akt compensated it. Uncoupling protein-2 (UCP-2) also plays a crucial role in the palmitate inhibition of insulin secretion, as confirmed by knockdown experiments, but SREBP-1c contribution to UCP-2 regulation was partial. The palmitate-EPA regulation of insulin secretion was similarly observed in islets from C57BL/6 mice pretreated with dietary manipulations. Furthermore, administration of EPA to diabetic KK-Ay mice ameliorated impairment of insulin secretion in their islets.

CONCLUSIONS—SREBP-1c plays a dominant role in palmitate-mediated insulin secretion defect, and EPA prevents it through SREBP-1c inhibition, implicating a therapeutic potential for treating diabetes related to lipotoxicity. ***Diabetes* 57:2382–2392, 2008**

From the [1]Department of Internal Medicine (Endocrinology and Metabolism), Graduate School of Comprehensive Human Sciences, University of Tsukuba, Tsukuba, Japan; the [2]Center for Tsukuba Advanced Research Alliance, University of Tsukuba, Tsukuba, Japan; and the [3]Department of Molecular Physiology and Biophysics, Vanderbilt University, Nashville, Tennessee.

Corresponding author: Hitoshi Shimano, shimano-tky@umin.ac.jp.

Received 29 December 2006 and accepted 23 April 2008.

Published ahead of print at http://diabetes.diabetesjournals.org on 5 May 2008. DOI: 10.2337/db06-1806.

Molecular mechanisms of pancreatic islet β-cell failure, a crucial pathological contributor to the development of diabetes, have been extensively explored (1–3). Impairment of glucose-stimulated insulin secretion (GSIS) is an early feature of type 2 diabetes, and influx of fatty acids into β-cells (β-cell lipotoxicity) has been thought to be involved in its pathogenesis (4,5). The intracellular events leading to GSIS include glucose metabolism for ATP production, closure of ATP-dependent K channels, membrane voltage-dependent calcium influx, calcium-dependent vesicle transport, and exocytosis of α-granules containing insulin (6,7). Lipotoxicity has been implicated in reducing GSIS via many of these steps (8). For example, uncoupling protein-2 (UCP-2), a mitochondrial membrane protein involved in energy production, plays an important role in fatty acid–induced lipotoxic effects (9–12). Although β-cells have traditionally been thought to simply produce insulin in response to glucose, more recent studies have highlighted the role of insulin signaling in β-cells. Studies on insulin signaling in β-cells, such as targeted disruption of the insulin receptor (13) and insulin receptor substrate-2 (IRS-2) (14,15), have shown that this pathway can influence both β-cell mass and insulin secretion.

Sterol regulatory element-binding protein (SREBP)-1c is a membrane-bound transcription factor of the basic helix loop helix leucine zipper family and has been established as a regulator of lipogenic enzymes in the liver (16,17). Expression of SREBP-1c is highly upregulated by dietary intake of carbohydrates and sugars (18–21). Conversely, polyunsaturated fatty acids (PUFAs), such as eicosapentaenoate (EPA), have been shown to inhibit hepatic SREBP-1c through multiple mechanisms (22,23). Recent data suggested that hepatic SREBP-1c is also induced by dietary saturated fatty acids (24). The data from SREBP-1c transgenic and LDL receptor knockout doubly mutant mice provide evidence that activation of this nutritionally regulated lipid transcription factor could be involved in formation of components of metabolic syndrome, such as hyperlipidemia and atherosclerosis (A. Takahashi, H. Shimano, unpublished data). Furthermore, SREBP-1c directly represses IRS-2 expression and leads to hepatic insulin resistance as a part of underlying pathogenesis for metabolic syndrome (25). In pancreatic β-cells, activation of SREBP-1c has been shown to be involved in impaired insulin secretion and glucose intolerance (26–28). Features of hepatic SREBP-1c induction by saturated fatty

acids, repression by PUFAs, and inhibition of IRS-2 were reproducibly observed in β-cells. As the major downstream insulin signaling pathway, the IRS-2/PI3K/Akt pathway has links to cell growth and survival and to glucose metabolism leading to ATP production (29). Insulin signaling in β-cells has been thought to be important for β-cell mass based on analyses of β-cell–specific transgenic mice of Akt (30–32) and tissue-specific knockout mice of insulin receptor (13) and IRS-2 (14,15). More recently, importance of insulin signaling in β-cell function has also been noticed in the glucose/insulin-signaling/Foxo1 pathway (29,33,34). Nuclear Foxo1 has a negative effect on β-cell mass and insulin secretion in vivo (34). Insulin signaling phosphorylates nuclear Foxo1 for nuclear exclusion and contributes to β-cell protection.

Recently, we reported that granuphilin, a crucial component of the docking machinery of insulin-containing vesicles to the plasma membrane (35–37), is regulated by SREBP-1c in β-cell (38). Thus, taken together with clinical implication of fatty acids as causative factors for β-cell lipotoxicity, it is conceivable that SREBP-1c is involved in β-cell lipotoxicity–mediated insulin secretion defects in GSIS.

In the current studies, we investigated the effects of palmitate, a typical saturated fatty acid, on GSIS in isolated islets and found that palmitate impairs GSIS and that addition of EPA protects against these effects. Analyses of palmitate-EPA on gene expression, including SREBP-1c and their target genes, led to clarification of the molecular mechanisms of palmitate-induced β-cell lipotoxicity and protective effects of EPA.

RESEARCH DESIGN AND METHODS

Palmitate and EPA were purchased from Sigma (St. Louis, MO). Enhanced chemiluminescence Western blot detection kit, [1-^{14}C]palmitate, and [^{3}H]mannitol were purchased from Amersham Biosciences.

This project was approved by the Animal Care Committee of the University of Tsukuba. Male C57BL/6 wild-type and KK-Ay mice at 8 weeks of age were purchased from Clea Japan (Tokyo). SREBP-1–null mice at 14–15 weeks of age were as described previously (39). The mice were housed in colony cages, maintained on a 12-h light/12-h dark cycle, given free access to water and a standard chow diet (MF; Oriental Yeast, Tokyo), and adapted to their new environment for 1 week before experiments.

Isolation of mouse pancreatic islets. Isolation of islets from mice was carried out according to the Ficoll-Conray protocol as described previously (26,38,40). In brief, after clamping the common bile duct at a point close to the duodenum outlet, 2.5 ml Krebs-Ringer bicarbonate buffer (KRBH, pH 7.4) containing 0.5% BSA and 4 mg/ml collagenase (Sigma) was injected into the duct. The swollen pancreas was removed and incubated at 37°C for 20 min. The pancreas was then dispersed by pipetting, and after washing twice with KRBH, the islets were collected manually under stereomicroscope. Isolated islets were put in culture medium (RPMI 1640 supplemented with 10% FCS, 0.5% BSA, 100 units/ml penicillin, and 100 μg/ml streptomycin as antibiotics) for 16–18 h at 37°C in a humidified atmosphere containing 5% CO_2 before the experiments.

Analyses of insulin secretion and insulin contents of islets. Insulin release from islets was measured as described previously (26,38). Batches of 10 islets were incubated for 30 min in 1 ml KRBH, pH 7.4, containing 0.5% BSA at 2.8 mmol/l glucose for 30 min. Islets medium was replaced with KRBH containing 20 mmol/l glucose or alternatively 30 mmol/l KCl plus 2.8 mmol/l glucose to estimate insulin secretion and were incubated for 30 min. At the end of each incubation period, the medium was collected, and islets were subjected to insulin extraction with acidic ethanol (0.2 mol/l HCl in 75% ethanol) for insulin measurement with an insulin enzyme-linked immunosorbent assay kit. Hoechst-33258 was used to determine the DNA contents of sonicated islets.

Determination of ATP-to-ADP ratio and triglyceride contents of islets. ATP and ADP contents in isolated islets were as described previously (26,38,41). ATP and ADP were extracted from islets with 5% of trichloroacetic acid. After centrifugation, the supernatants were neutralized with NaOH. ATP content was measured using the CellTiter-Glo luminescent cell viability assay kit (Promega, Madison, WI). ADP content was estimated after conversion of ADP to ATP in the reaction buffer (20 mmol/l HEPES and 3 mmol/l $MgCl_2$, pH 7.75) containing 2.3 units/ml pyruvate kinase and 1.5 mmol/l phosphoenolpyruvate at room temperature for 15 min.

Triglycerides (TGs) of islets were measured after extracting lipids with Folch's method. After 1–2 min of sonication, islets were mixed with chloroform and methanol (2:1) for lipid extraction, dried up by evaporation, and resuspended in isopropanol. TG concentration was measured using the GPO-trinder kit (Sigma).

Real-time PCR and immunoblot analysis. Total RNA extraction with the TRIzol reagent (Invitrogen, Carlsbad, CA) and DNase-I treatment using the RNeasy Micro kit (Qiagen, Hilden, Germany) were performed according to the manufacturers' instructions. cDNA was synthesized with ThermoScript (Invitrogen), and comparative analysis of mRNA levels was performed with fluorescence-based real-time PCR. Real-time PCR analyses were performed using SYBR-Green Dye (Nippon Gene, Tokyo) in an ABI 7000 PCR instrument (Applied Biosystems, Foster City, CA). The relative abundance for each transcript was calculated by a standard curve of cycle thresholds for serial dilutions of a cDNA sample and normalized to cyclophilin. Primer sequences are described in supplemental Table 3, which is available in the online appendix at http://dx.doi.org/10.2337/db06-1806.

Immunoblot analyses were performed as described previously (26,38). Cell extracts from isolated islets were probed with rabbit polyclonal anti–SREBP-1 (sc-8984; Santa Cruz Biotechnology, Santa Cruz, CA), anti–IRS-2 (06–506; Upstate Technology, Bedford, MA), anti-Akt (no. 9272), anti–phospho Akt (S473; no. 9271), anti–phospho Akt (T308; no. 9275; Cell Signaling, Beverly, MA), anti–UCP-2 (Research Diagnostic, San Antonio, TX), and anti–α-tubulin (sc-8035; Santa Cruz Biotechnology). Anti-granuphilin a/b antibody was used as previously described (37,38). Detection was performed using an ECL advance Western blotting detection kit and ECL Hyperfilm (Amersham Biosciences).

Treatment of islets with palmitate and EPA. Palmitate and EPA were dissolved to 100 mmol/l in methanol to make stock solutions for later dilution in RPMI 1640 supplemented with 0.5% BSA to a final concentration of 400 μmol/l (palmitate) and 50 μmol/l (EPA), respectively. Islets were treated for 48 h before indicated experiments.

Cellular uptake of [1-^{14}C]palmitate. [1-^{14}C]palmitate uptake of islets was measured as described previously (42). Briefly, the isolated islets were incubated for 60 min in culture medium containing 400 μmol/l palmitate, 0.3 μCi/ml radiolabeled [1-^{14}C]palmitate with or without 50 μmol/l EPA, and 0.06 μCi/ml [^{3}H]mannitol. The latter was used to calculate correction for nonspecific uptake. Ice-cold 0.5 N NaOH was added to the islets to terminate the uptake reaction and neutralized by 0.5 N HCl. After the removal of the supernatant by centrifugation at 12,000 × *g* for 1 min, the residual radioactivity was determined.

Small interfering RNA for UCP-2. The small interfering RNA (siRNA) construct for mouse UCP-2 was generated within the coding region of UCP-2: 5′-GTCGAAGCCTACAAGACCA-3′ (Ad-UCP-2 RNAi). The siRNA for LacZ (Ad-LacZ RNAi) from Invitrogen (BLOCK-iT U6 RNAi Entry Vector kit; K4944–00) was used as a control according to manufacturer's instructions. Oligonucleotide containing this sequence was subcloned into U6/RNAi Entry vector (Invitrogen). UCP-2 RNAi adenoviruses were generated using BLOCK-iT Adenoviral RNAi Expression System (Invitrogen).

Adenovirus infections for constitutively active Akt and siRNA of UCP2. Infection of constitutively active Akt (43) and siRNA of UCP-2 adenovirus studies were performed as described previously (25,38,44). In brief, generation of recombinant adenoviral plasmid was produced by homologous recombination with the pAdEasy-1 plasmid (Invitrogen). Production of recombinant adenoviruses was performed by CsCl gradient centrifugation as previously described (25,38,44).

Palmitate-rich diet study and KK-Ay mice study. The in vivo palmitate-rich diet study and KK-Ay mice study were described in RESEARCH DESIGN AND METHODS in the online appendix. Briefly, in the palmitate-rich diet study, C57BL6 mice were fed with control diet (fish oil–free diet), tripalmitin diet (20% tripalmitin), and tripalmitin plus EPA-E diet (20% tripalmitin and 5% EPA-E) for 28 days. In KK-Ay mice study, KK-Ay mice were administered vehicle (5% gum arabic) or EPA-E at a dose of 1 g · kg^{-1} · day^{-1} for 28 days.

Statistical analysis. Results are reported as means ± SE. Statistical analyses were performed using one-way ANOVA followed by Dunnett's procedure or two-way ANOVA followed by Tukey's procedure.

RESULTS

Palmitate impairs and EPA restores insulin secretion in murine islets. To investigate pancreatic lipotoxicity, we evaluated effects of palmitate (C16:0) on the insulin

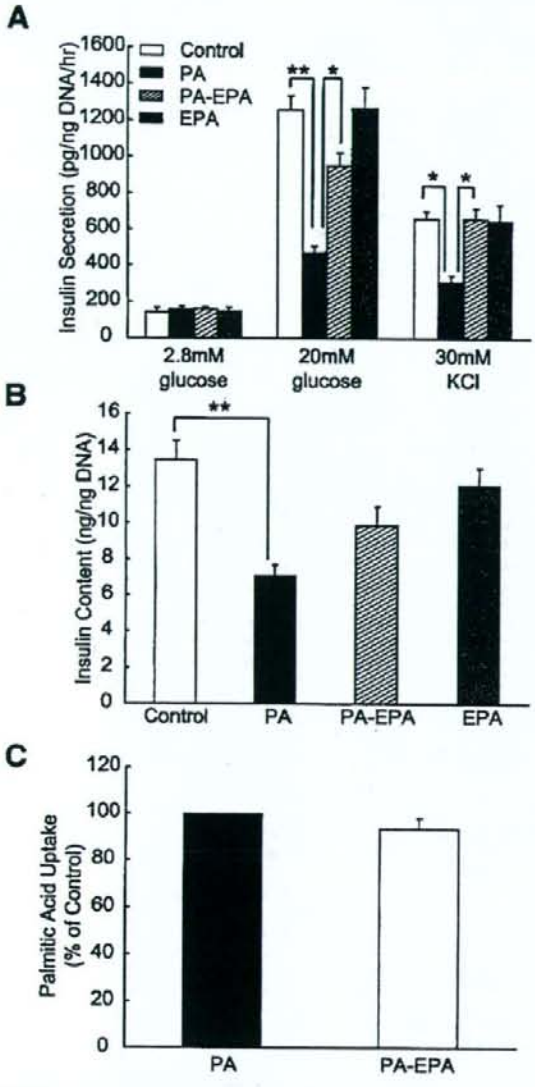

FIG. 1. Lipotoxic effects of palmitate and protective effects of EPA on insulin secretion in murine-isolated islets. *A*: Low GSIS (2.8 mmol/l), high GSIS (20 mmol/l), and KSIS from murine-isolated islets incubated without (control, white bars) or with palmitate (black bars), palmitate-EPA (bold hatched bars), or EPA (regular hatched bars). *B*: Insulin content of islets incubated without (control) or with palmitate, palmitate-EPA, or EPA. *C*: Palmitate uptake in islets isolated from C57BL/6 mice. Three independent experiments were performed using four sets of islets for each repetition, and results are expressed as means ± SE. Statistical analysis was performed using one-way ANOVA followed by Dunnett's procedure. $^{**}P < 0.01$ and $^{*}P < 0.05$ vs. palmitate group, respectively.

secretion of isolated mouse pancreatic islets. Although palmitate (400 μmol/l) had no effect on basal insulin secretion (low glucose concentrations), stimulation with high glucose concentrations, i.e., GSIS, was inhibited by the addition of palmitate (Fig. 1*A*). When 50 μmol/l EPA (C20:5, n-3) was combined with palmitate-treated islets (hereafter referred to as palmitate-EPA), the suppressed insulin secretion was restored to near-normal levels (Fig. 1*A*). Palmitate inhibition and EPA restoration of insulin secretion was also observed after addition of KCl, which bypasses ATP-sensitive channels to stimulate insulin secretion (KCl-stimulated insulin secretion [KSIS]) (Fig. 1*A*). These effects of palmitate and EPA on insulin secretion were dose dependent (supplemental Fig. 1*A* and *B*). EPA by itself did not have any effect on GSIS or KSIS, indicating that EPA does not intrinsically increase but cancels palmitate-suppressed insulin secretion. The slight changes of insulin content compared with GSIS and KSIS by palmitate and EPA indicate that the phenomenon in insulin content was only a part of the mechanism (Fig. 1*B*). Considering the experimental setting, the protective effect of EPA against palmitate-induced lipotoxicity could be inhibition of cellular uptake of palmitate. To exclude this possibility, uptake of labeled palmitate was measured and was not affected by additional EPA (Fig. 1*C*). These data indicate that the EPA does not interfere with palmitate uptake but rather directly competes with palmitate in intracellular events.

Palmitate and EPA regulate SREBP-1c and its target genes. Gene expression in palmitate- and palmitate-EPA–treated islets was investigated using real-time PCR. SREBP-1c mRNA was highly induced by palmitate and completely suppressed by EPA but not SREBP-1a mRNA (Fig. 2*A*). These changes in SREBP-1c mRNA were associated with those in both membrane and nuclear forms of SREBP-1c protein (Fig. 2*D*). In accordance, its target genes, such as fatty acid synthase, stearoy-CoA desaturase 1, and elongation of long-chain fatty acids family number 6 showed similar patterns of regulation by palmitate and palmitate-EPA (Fig. 2*B*). TG content, as an indication of SREBP-1c effect and lipotoxicity, was increased by palmitate and repressed by palmitate-EPA (Fig. 2*C*).

We recently reported that SREBP directly suppressed hepatic IRS-2 expression and caused insulin resistance in the liver (25). In accordance with changes in SREBP-1c in islets, IRS-2 was strongly suppressed by palmitate and was partially restored by addition of EPA, implicating a role for SREBP-1c–mediated IRS-2 repression in the palmitate-EPA–mediated changes in β-cell physiology (Fig. 2*D*; supplemental Fig. 2*A*).

UCP-2 has been shown to play a key role in lipotoxicity of pancreatic β-cells through dissociation of fatty acid oxidation and ATP production (supplemental Fig. 2*B*) (9–12). UCP-2 promoter was also reported as an SREBP target (11,12). This key regulator of lipotoxicity was modulated by palmitate and palmitate-EPA in a similar manner at both mRNA and protein levels (supplemental Fig. 2*A*; Fig. 2*D*).

Granuphilin was an effector of Rab27a, and its overexpression was reported to inhibit exocytosis of insulin granules (35–37). We recently reported that granuphilin promoter was a direct target of SREBP-1c and that the SREBP-1c/granuphilin pathway was a potential mechanism for impairment GSIS in diabetes, leading to β-cell lipotoxicity (38). This key molecule of lipotoxicity was upregulated by palmitate and suppressed by palmitate-EPA at both mRNA and protein levels (supplemental Fig. 2*A*; Fig. 2*D*).

SREBP-1c plays a dominant role in palmitate-EPA effects on insulin secretion. The contribution of SREBP-1c to palmitate-EPA effects on both GSIS and KSIS was estimated using islets from SREBP-1–null mice. Basal insulin secretion was not affected by SREBP-1 deficiency (data not shown); however, GSIS was modestly increased

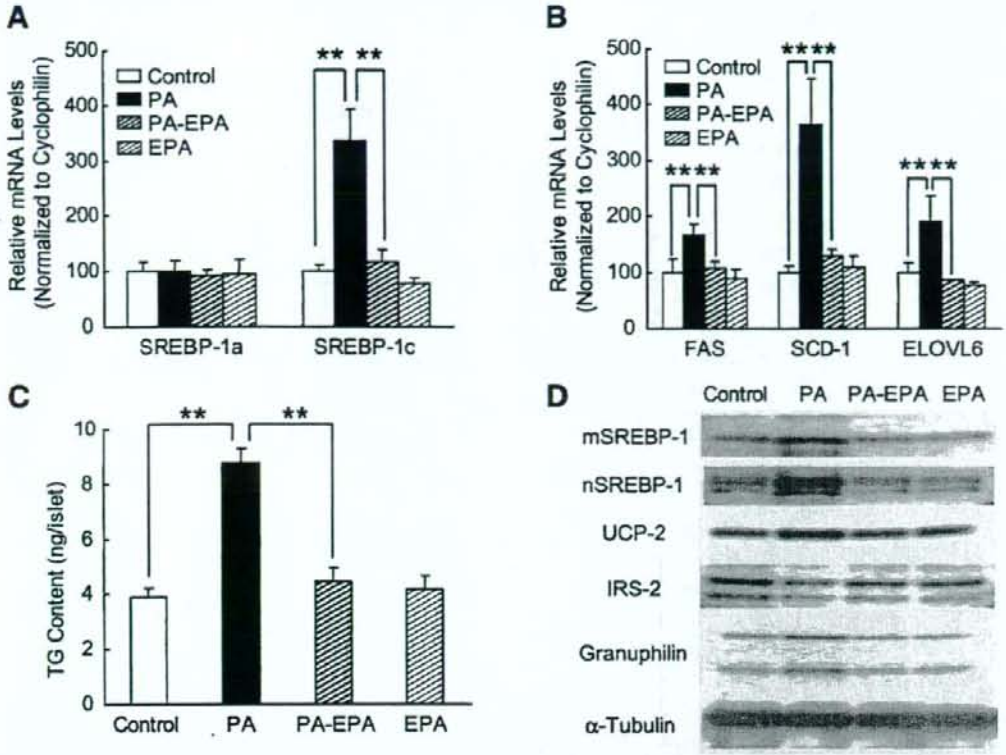

FIG. 2. Gene expression and protein profiles in murine-isolated islets treated with palmitate or palmitate-EPA. *A* and *B*: Levels of mRNA of various genes in pancreatic islets isolated from C57BL/6 mice without (control, white bars) or with palmitate (black bars), palmitate-EPA (hatched bars), or EPA (regular hatched bars) as determined by real-time PCR. mRNA quantities were calculated as a ratio to the cyclophilin level in the each cDNA sample. Data are shown as the relative expression ratio to control samples. *C*: Cellular TG levels of islets incubated with palmitate, palmitate-EPA, or EPA. *D*: Immunoblot analysis of indicated proteins in the islets. Cont., control; mSREBP-1, membrane form of SREBP-1; nSREBP-1, nuclear form of SREBP-1. α-Tubulin protein was used as a loading control. Three independent experiments were performed using four sets of islets, and results are expressed as means ± SE. Statistical analyses were performed using one-way ANOVA followed by Dunnett's procedure. **$P < 0.01$ vs. palmitate group.

(Fig. 3*A*). The absence of SREBP-1 abolished palmitate-induced inhibition of GSIS and KSIS (Fig. 3*A*). Because of this, EPA protection from impairment of GSIS and KSIS, as observed in wild-type islets, was not detected in SREBP-1–null islets (Fig. 3*A*). These data suggest that palmitate-induced pancreatic lipotoxicity and amelioration of that by EPA depend on SREBP-1c. Predictably, from the primary role of SREBP-1c in lipogenesis, the elevation and repression of TG content in wild-type islets by palmitate and EPA, respectively, were absent in SREBP-1–null islets (Fig. 3*B*). Suppression of IRS-2 and stimulation of granuphilin mRNA expressions caused by palmitate in wild-type islets were both blunted in SREBP-1–null islets (Fig. 4*A*). Accordingly, the reversal of palmitate effects on IRS-2 and granuphilin expression by EPA was not observed in SREBP-1–null islets. On the other hand, induction of UCP-2 expression by palmitate was observed even in SREBP-1–null islets, but EPA treatment reversed the palmitate effect in both genotypes (Fig. 4*A*).

IRS-2 suppression by SREBP-1c contributes to palmitate-EPA effects on GSIS. Based on recent cumulative evidence of the importance of insulin signaling in β-cell function and our observation of reciprocal changes in SREBP-1c and IRS-2 by addition of palmitate and/or EPA in islets (Fig. 2*D*; supplemental Fig. 2*A*), we hypothesized that palmitate suppression of insulin secretion might be due to impaired insulin signaling caused by induction of SREBP-1c, leading to decreased IRS-2 expression. To test this hypothesis, insulin signaling was estimated in wild-type and SREBP-1–null islets by analysis of Akt phosphorylation status. Consistent with changes at the mRNA level (supplemental Fig. 2*A*), suppression and restoration of IRS-2 protein by palmitate and palmitate-EPA, respectively, in wild-type islets was not apparent in SREBP-1–null islets (Fig. 4*B*). Consequently, Akt phosphorylation impaired by palmitate in wild-type islets was completely abolished by the absence of SREBP-1 (Fig. 4*B*). These data suggest that SREBP-1c could be highly involved in palmitate-mediated inhibition of insulin signaling and insulin secretion.

To explore impacts of insulin signaling on palmitate-EPA–regulated insulin secretion, forced activation of insulin signaling downstream of IRS-2 was induced in mouse isolated islets by adenoviral gene transfer of constitutively active (dominant-positive) Akt (Akt-CA). Akt-CA overexpression significantly improved both GSIS and KSIS, which were impaired by palmitate, but did not further enhance restoration by EPA, indicating that insulin signaling and insulin secretion were linked in palmitate-EPA effects (Fig. 5*A*). Akt-CA overexpression only slightly

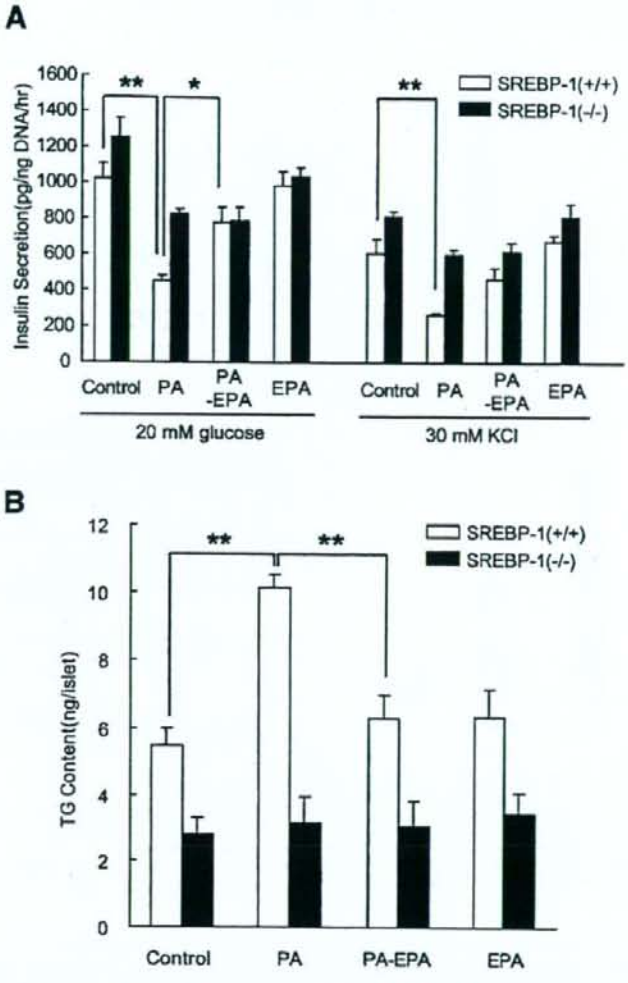

FIG. 3. Protection from palmitate-induced lipotoxicity in islets isolated from SREBP-1–null mice. Islets were isolated from wild-type littermates (white bars) and SREBP-1–null mice (black bars) and incubated without (control) or with palmitate, palmitate-EPA, or EPA for 48 h. GSIS and KSIS (*A*) and cellular TG contents (*B*) were measured. Three independent experiments were performed using four sets of islets, and results are expressed as means ± SE. Statistical analyses were performed using two-way ANOVA followed by Tukey's procedure. **$P < 0.01$ and *$P < 0.05$, respectively.

enhanced phosphorylation of Akt in untreated islets but completely restored suppressed pAkt in palmitate-treated islets (Fig. 5*B*). Insulin signaling downstream of Akt, such as pAkt, was also consistently suppressed by palmitate. These signaling molecules were all restored by Akt-CA overexpression. Islets treated with palmitate-EPA exhibited signals similar to control islets regardless of Akt-CA overexpression (Fig. 5*B*). Both SREBP-1 deficiency (Figs. 3*A* and 4*B*) and constitutive activation of insulin signaling by Akt-CA (Fig. 5*A* and *B*) cancelled the protective effects of EPA against palmitate-induced impaired insulin secretion and insulin signaling. Activation of Akt did not change either SREBP-1c or UCP-2 (Fig. 5*C*).

Contribution of UCP-2 to palmitate-EPA effects on GSIS. The contribution of UCP-2 to the effects of palmitate-EPA on GSIS was estimated in knockdown experiments using adenoviral siRNA of UCP-2. A robust inhibition of mRNA and protein levels of UCP-2 was obtained (Fig. 6*A*; supplemental Fig. 3). Gene silencing of UCP-2 did not effect basal insulin secretion or GSIS. In contrast, UCP-2 knockdown significantly protected palmitate-mediated impaired GSIS and canceled the EPA protection (Fig. 6*B*). Palmitate-mediated reduction in ATP-to-ADP ratio was significantly restored by UCP-2 suppression, and the protective effect of EPA was also canceled (Fig. 6*C*). Changes in ATP-to-ADP ratio and GSIS by modulation of UCP-2 expression were very similar, confirming that the palmitate-EPA effects on GSIS depend on the UCP-2/ATP system, as was previously suggested by knockout mice studies. Palmitate induction of SREBP-1c was not affected by UCP-2 knockdown (Fig. 6*D*). Taken together with partial regulation of UCP-2 in SREBP-1–null islets (Fig. 4*A*), effects of UCP-2 and SREBP-1c on GSIS are partially connected.

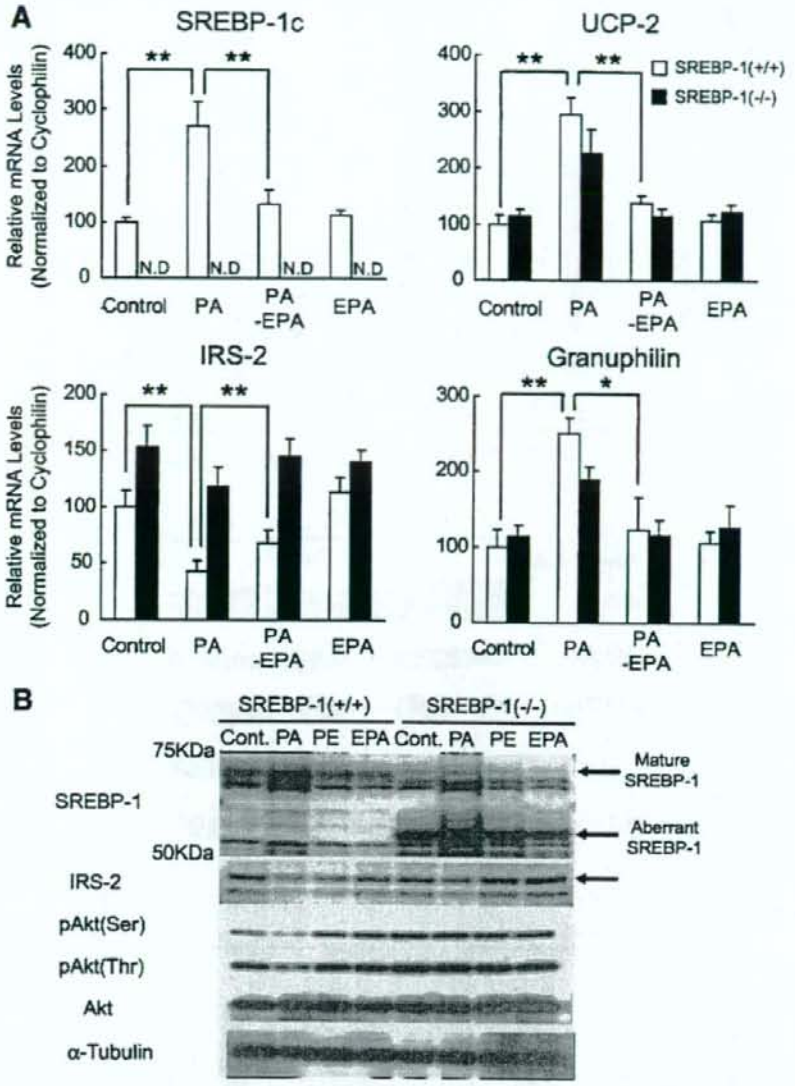

FIG. 4. Gene expression and protein profiles in islets isolated from SREBP-1–null mice treated with palmitate or palmitate-EPA. Islets were isolated from SREBP-1–null mice and wild-type littermates and incubated without (control) or with palmitate, palmitate-EPA (PE), or EPA for 48 h. *A*: mRNA levels of the indicated genes were measured. mRNA levels were determined by real-time PCR, calculated as ratio to cyclophilin expression levels. *B*: Immunoblot analysis of SREBP-1 and insulin-signaling proteins. Relative expression ratios to control samples are shown. Three independent experiments were performed using four sets of islets, and results are expressed as means ± SE. Statistical analyses were performed using two-way ANOVA followed by Tukey's procedure. **$P < 0.01$ and *$P < 0.05$, respectively.

EPA in vivo exhibits a protective role against palmitate lipotoxicity in islets. To determine whether the effects of palmitate-EPA on GSIS in isolated islets could be extended in vivo, mice were fed a fish oil–free diet with or without 20% tripalmitin or tripalmitin plus 5% EPA ethyl ester for 28 days, and GSISs in freshly isolated islets from these animals were measured. Palmitate feeding impaired and EPA restored GSIS in conjunction with changes in islet SREBP-1c expression (Fig. 7*A* and *B*). These data demonstrate that dietary palmitate and EPA influence insulin secretion in vivo in a similar manner to palmitate-EPA effects observed in isolated islets.

The effect of EPA on GSIS in vivo was further investigated in isolated islets from KK-Ay mice, a model of obesity and type 2 diabetes (45). In islets from KK-Ay mice, GSIS was impaired, and SREBP-1c expression was increased. Administration of EPA ethyl ester at a dose of $1\ g \cdot kg^{-1} \cdot day^{-1}$ for 28 days restored GSIS and suppressed SREBP-1c expression (Fig. 7*C* and *D*), leading to restoration of GSIS and KSIS. In both in vivo experiments, these data did not accompany changes in food intake or gross morphological changes in pancreatic islets (supplemental Tables 1 and 2; Fig. 4).

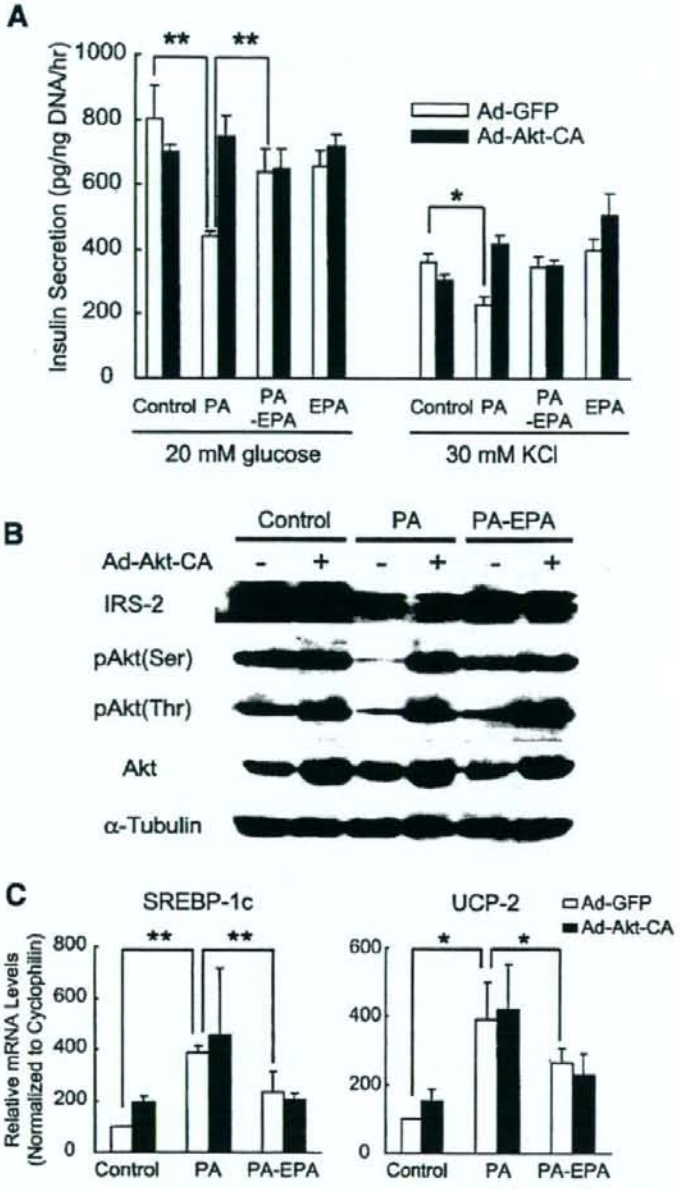

FIG. 5. Effects of overexpression of constitutively active Akt in islets treated with palmitate or palmitate-EPA. Islets were isolated from C57BL/6 mice and incubated without (control) or with palmitate or palmitate-EPA for 48 h. Islets were infected (100 multiplicity of infection, respectively) with adenoviral-GFP (Ad-GFP) or adenoviral–constitutively active Akt (Ad-Akt-CA) for 48 h before incubation with palmitate or palmitate-EPA. GSIS and KSIS (*A*) and protein levels of indicated insulin-signaling molecules (*B*) were measured. Amounts of insulin-signaling proteins were estimated by immunoblot analysis using indicated antibodies, and α-tubulin protein was used as a loading control. Levels of mRNA of SREBP-1c and UCP-2 were determined by real-time PCR (*C*), calculated as ratio to cyclophilin expression levels. Relative expression ratios to control samples are shown. Three independent experiments were performed using four sets of islets, and results are expressed as means ± SE. Statistical analyses were performed using two-way ANOVA followed by Tukey's procedure. **$P < 0.01$ and *$P < 0.05$, respectively.

DISCUSSION

It has long been known that chronic exposure of palmitate to islets or β-cell lines causes lipotoxicity leading to blunted GSIS (1,3–5). Our current studies clearly demonstrate that this palmitate-induced impairment of insulin secretion is restored by supplement of EPA. The results also indicated that this palmitate-EPA regulation is not due to cell toxicity or apoptosis (data not shown) but mediated through two major key molecules: SREBP-1c and UCP-2. Several factors are known to be important for function of

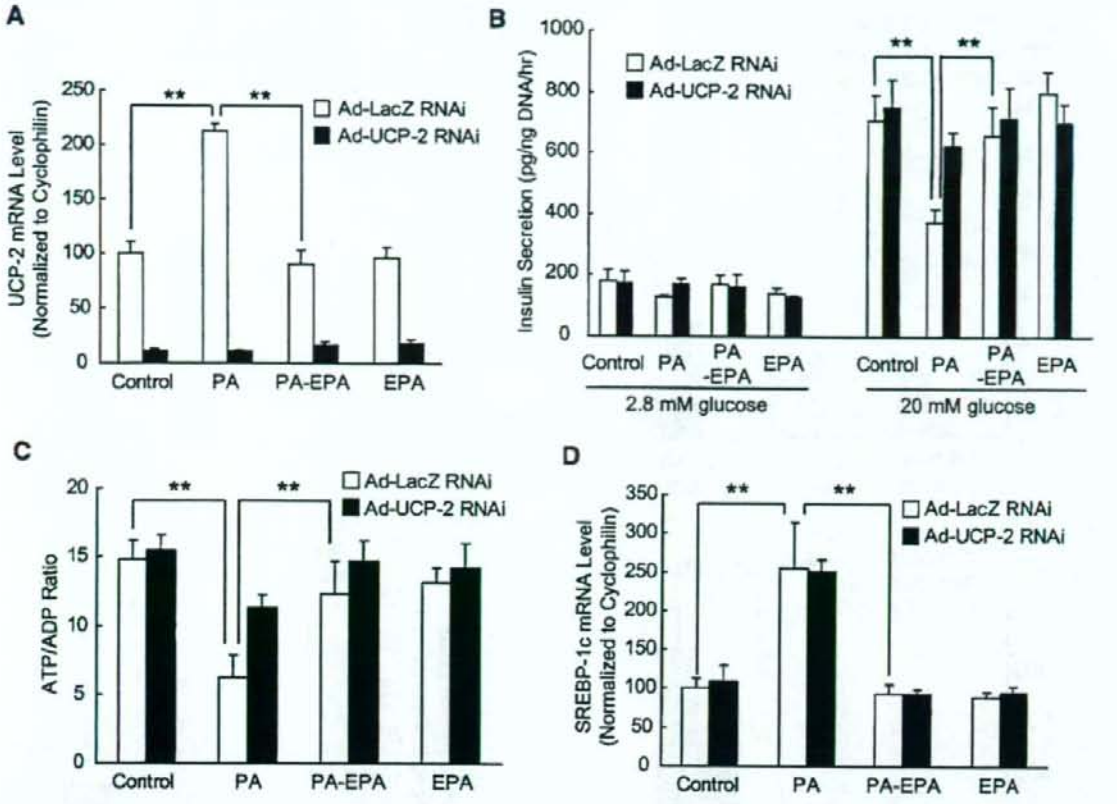

FIG. 6. Effects of UCP-2 gene silencing on murine-isolated islets treated with palmitate or palmitate-EPA. Islets were isolated from C57BL/6 mice and infected (500 multiplicity of infection, respectively) with adenoviral siRNA for LacZ (Ad-LacZ RNAi) or UCP-2 (Ad-UCP-2 RNAi) and cultured without (control) or with palmitate, palmitate-EPA, or EPA for 48 h. *A*: The effects of UCP-2 siRNA on mRNA levels of UCP-2 in pancreatic islets isolated from C57BL/6 mice incubated with palmitate, palmitate-EPA, or EPA were determined by real-time PCR. GSIS (*B*) and ATP-to-ADP ratio (*C*) from the islets after UCP-2 gene silencing and incubation with palmitate, palmitate-EPA, or EPA were measured. Level of mRNA of SREBP-1c was determined by real-time PCR (*D*), calculated as ratio to cyclophilin expression levels. Relative expression ratios to control samples are shown. Three independent experiments were performed using four sets of islets, and results are expressed as means ± SE. Statistical analyses were performed using two-way ANOVA followed by Tukey's procedure. **$P < 0.01$.

β-cells, such as ATP-to-ADP ratio, IRS-2/Akt insulin signaling, and granuphilin. These factors are all consistently disturbed by palmitate and improved by additional EPA through up- and downregulation of SREBP-1c, respectively. Taken together with overexpression and knockout experiments of SREBP-1, it can be concluded that SREBP-1c plays a crucial role in β-cell lipotoxicity as a causative upstream factor.

Contribution of UCP-2 to ATP depletion and impaired insulin secretion has been well established (9–12,26). Our current studies also confirm this in palmitate-mediated suppression of GSIS. Palmitate led to upregulation of UCP-2 and reduction of intracellular ATP. Knockdown of UCP-2 by siRNA restored palmitate-induced impairment of GSIS. SREBP has been reported to directly bind to and activate the UCP-2 promoter (11,12). Supportively, we observed that β-cell–specific overexpression of SREBP-1c elevated UCP-2 expression contributing to the β-cell lipotoxicity in transgenic mice (26). However, based on the current results from SREBP-1–null islets, SREBP-1c only partially participated in palmitate-induced expression of UCP-2. Conversely, UCP-2 knockdown did not affect SREBP-1c expression in islets. Thus, although both key molecules play a dominant role in β-cell lipotoxicity, there might not be a definite causative relationship between SREBP-1c, an indicator of lipogenesis, and UCP-2, an indicator of energy consumption (Fig. 8).

Our data on Akt-CA overexpression experiments provide further evidence for the importance of insulin signaling in β-cell function. Palmitate inhibited and EPA restored insulin signaling in an opposite manner to SREBP-1c expression. Based on the potential effect of SREBP-1c on insulin signaling through regulation of IRS-2 (25,26), we explored involvement of insulin signaling in palmitate-EPA regulation of insulin secretion. Activation of Akt did not change normal insulin secretion but markedly ameliorated palmitate-impaired insulin secretion in isolated islets. Thus, insulin signaling could be a prerequisite for insulin secretion, and the importance of its role in insulin secretion becomes overt only with regard to its impairment. Palmitate suppression of insulin signaling was cancelled in SREBP-1–null islets. Based on these data, we conclude that SREBP-1c in β-cells plays a crucial role in the inhibition of insulin signaling via suppression of IRS-2 and contributes to impaired insulin secretion (26). In contrast to established effects of insulin signaling on β-cell

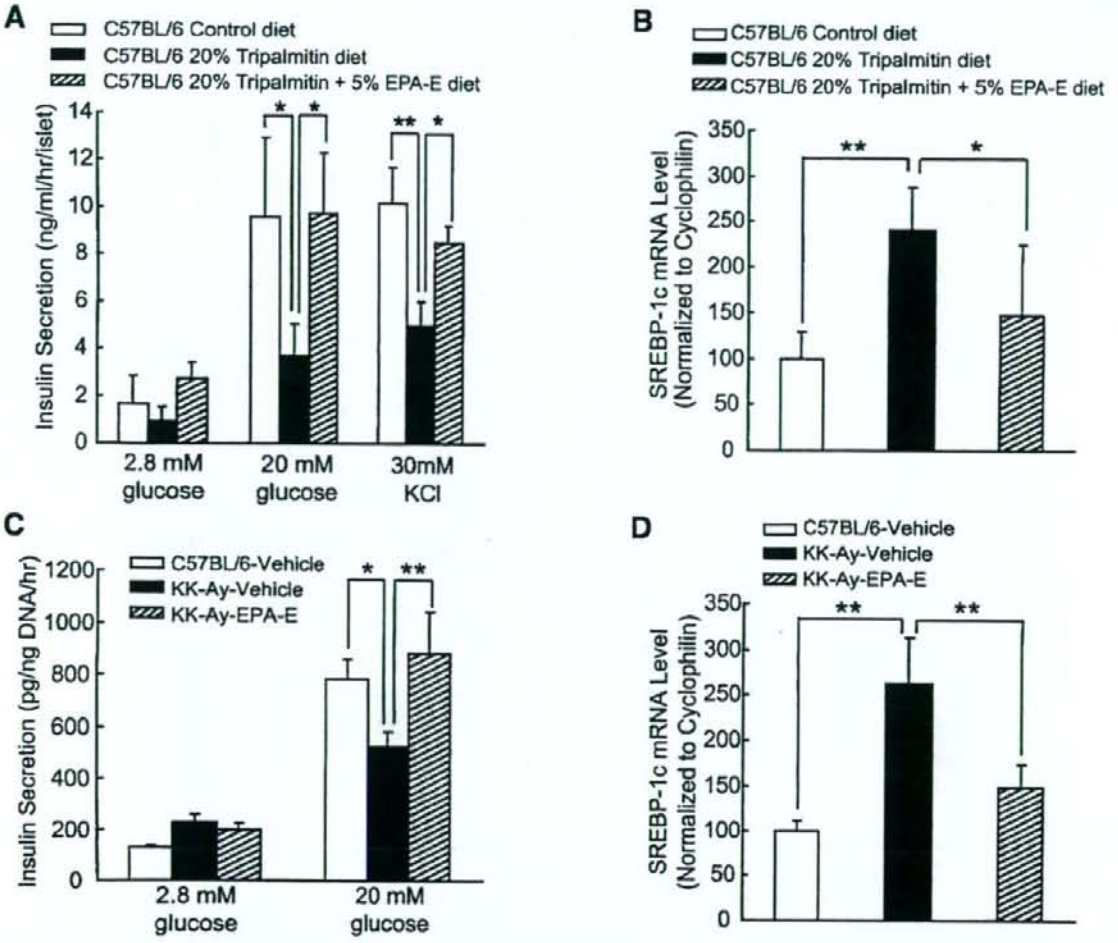

FIG. 7. Effect of EPA on insulin secretion in vivo. C57BL/6 mice were fed control diet (white bars), 20% Tripalmitin diet (black bars), and Tripalmitin + 5% EPA-E diet (hatched bars) for 28 days. Islets were isolated from individual animals. GSIS and KSIS (*A*) and mRNA levels of SREBP-1c (*B*) were measured. KK-Ay mice were administered vehicle (black bars) or EPA at a dose of 1 $g \cdot kg^{-1} \cdot day^{-1}$ (hatched bars) for 28 days. Islets were isolated from pool pancreas (three to four animals). GSIS (*C*) and mRNA levels of SREBP-1c (*D*) were measured. Three independent experiments were performed using four sets of islets, and results are expressed as means ± SE. Statistical analyses between indicated groups were performed using one-way ANOVA followed by Dunnett's procedure. **$P < 0.01$ and *$P < 0.05$, respectively.

mass (13–15,29–34), our data indicated that activation of Akt could restore insulin secretion impaired by palmitate in a short term. The precise molecular mechanism for this is currently unknown, although phosphorylation of Foxo-1 and anti-apoptosis could be involved (29,34).

Dietary PUFAs, such as EPA, have been shown to have plasma TG-lowering effects and to improve fatty liver and hepatic insulin resistance (22,23,46). We previously reported that PUFAs inhibited hepatic SREBP-1c, which contributed to beneficial roles of PUFAs against lipotoxicity in the liver (22,23). Current data provide another beneficial role of EPA: protection from lipotoxicity in pancreatic β-cells. Our data also suggest that this protective action of EPA is mediated mainly through suppression of SREBP-1c. EPA reduced mRNA and nuclear protein levels of SREBP-1c in palmitate-treated islet. In addition, a large portion of EPA protection against palmitate-induced impaired GSIS was not reproduced in SREBP-1–null islets. Amelioration of impaired GSIS by EPA was also confirmed in vivo with SREBP-1c suppression. EPA also suppressed overexpression of UCP-2 by palmitate even in SREBP-1–null islets. This suggests that suppression of UCP-2 also may contribute to protective effect of EPA against palmitate-mediated suppression of GSIS, which is presumably independent of SREBP-1c (Fig. 7).

Our data showing that enhancement of insulin signaling in β-cells can improve impaired insulin secretion caused by lipotoxic effects of palmitate have important clinical relevance. It has been recognized that hyperglycemia exacerbates the impairment of insulin secretion, often referred to as glucotoxicity, and that short-term insulin treatment often effectively improves insulin secretion. This has been thought to be due to reducing blood glucose; however, our current findings implicate that stimulation of insulin signaling in β-cells could potentially contribute to the improvement of insulin secretion, especially in lipo-

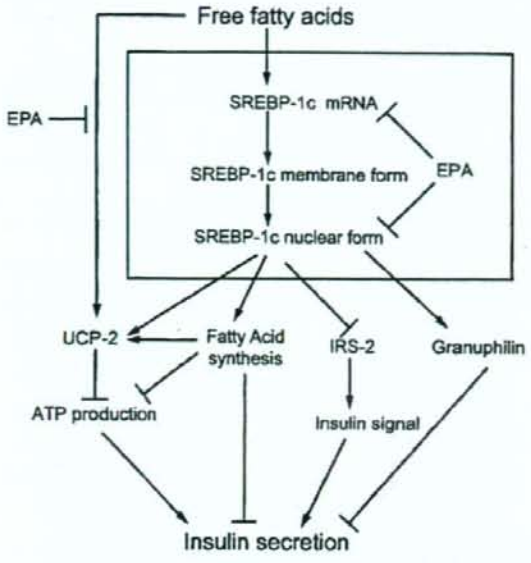

FIG. 8. Mechanism by which palmitate induces and EPA protects impairment of insulin secretion in pancreatic islets.

toxic states. From a long-term standpoint, our findings might relate to the onset of type 2 diabetes because intake of excess saturated fatty acids can cause both insulin resistance and impaired insulin secretion in β-cells. Our data also suggest that oral dosing of EPA could contribute to protection from the β-cell lipotoxicity. Because our findings are based mostly on in vitro studies, further investigations in vivo are needed to test our conclusions.

ACKNOWLEDGMENTS

This research was partially supported by the Ministry of Education, Science, Sports, and Culture Grant-in-Aid for Scientific Research.

REFERENCES

1. Kahn SE: Clinical review 135: the importance of beta-cell failure in the development and progression of type 2 diabetes. *J Clin Endocrinol Metab* 86:4047–4058, 2001
2. Weir GC, Bonner-Weir S: Five stages of evolving β-cell dysfunction during progression to diabetes. *Diabetes* 53 (Suppl. 3):S16–S21, 2004
3. Stumvoll M, Goldstein BJ, van Haeften TW: Type 2 diabetes: principles of pathogenesis and therapy. *Lancet* 365:1333–1346, 2005
4. Unger RH: Lipotoxicity in the pathogenesis of obesity-dependent NIDDM: genetic and clinical implications. *Diabetes* 44:863–870, 1995
5. Boden G, Shulman GI: Free fatty acids in obesity and type 2 diabetes: defining their role in the development of insulin resistance and beta-cell dysfunction. *Eur J Clin Invest* 32 (Suppl. 3):14–23, 2002
6. Rorsman P, Renstrom E: Insulin granule dynamics in pancreatic beta cells. *Diabetologia* 46:1029–1045, 2003
7. Prentki M, Tornheim K, Corkey BE: Signal transduction mechanisms in nutrient-induced insulin secretion. *Diabetologia* 40 (Suppl. 2):S32–S41, 1997
8. Girard J: [Contribution of free fatty acids to impairment of insulin secretion and action. mechanism of beta-cell lipotoxicity]. *Med Sci (Paris)* 21:19–25, 2005
9. Chan CB, Saleh MC, Koshkin V, Wheeler MB: Uncoupling protein 2 and islet function. *Diabetes* 53 (Suppl. 1):S136–S142, 2004
10. Joseph JW, Koshkin V, Saleh MC, Sivitz WI, Zhang CY, Lowell BB, Chan CB, Wheeler MB: Free fatty acid-induced beta-cell defects are dependent on uncoupling protein 2 expression. *J Biol Chem* 279:51049–51056, 2004
11. Yamashita T, Eto K, Okazaki Y, Yamashita S, Yamauchi T, Sekine N, Nagai R, Noda M, Kadowaki T: Role of uncoupling protein-2 up-regulation and triglyceride accumulation in impaired glucose-stimulated insulin secretion in a beta-cell lipotoxicity model overexpressing sterol regulatory element-binding protein-1c. *Endocrinology* 145:3566–3577, 2004
12. Medvedev AV, Robidoux J, Bai X, Cao W, Floering LM, Daniel KW, Collins S: Regulation of the uncoupling protein-2 gene in INS-1 beta-cells by oleic acid. *J Biol Chem* 277:42639–42644, 2002
13. Kulkarni RN, Bruning JC, Winnay JN, Postic C, Magnuson MA, Kahn CR: Tissue-specific knockout of the insulin receptor in pancreatic beta cells creates an insulin secretory defect similar to that in type 2 diabetes. *Cell* 96:329–339, 1999
14. Lin X, Taguchi A, Park S, Kushner JA, Li F, Li Y, White MF: Dysregulation of insulin receptor substrate 2 in beta cells and brain causes obesity and diabetes. *J Clin Invest* 114:908–916, 2004
15. Kubota N, Terauchi Y, Tobe K, Yano W, Suzuki R, Ueki K, Takamoto I, Satoh H, Maki T, Kubota T, Moroi M, Okada-Iwabu M, Ezaki O, Nagai R, Ueta Y, Kadowaki T, Noda T: Insulin receptor substrate 2 plays a crucial role in beta cells and the hypothalamus. *J Clin Invest* 114:917–927, 2004
16. Shimano H, Horton JD, Hammer RE, Shimomura I, Brown MS, Goldstein JL: Overproduction of cholesterol and fatty acids causes massive liver enlargement in transgenic mice expressing truncated SREBP-1a. *J Clin Invest* 99:1575–1584, 1996
17. Shimano H, Horton JD, Shimomura I, Hammer RE, Brown MS, Goldstein JL: Isoform 1c of sterol regulatory element binding protein is less active than isoform 1a in livers of transgenic mice and in cultured cells. *J Clin Invest* 99:846–854, 1997
18. Shimano H, Yahagi N, Amemiya-Kudo M, Hasty AH, Osuga J, Tamura Y, Shionoiri F, Iizuka Y, Ohashi K, Harada K, Gotoda T, Ishibashi S, Yamada N: Sterol regulatory element-binding protein-1 as a key transcription factor for nutritional induction of lipogenic enzyme genes. *J Biol Chem* 274:35832–35839, 1999
19. Hasty AH, Shimano H, Yahagi N, Amemiya-Kudo M, Perrey S, Yoshikawa T, Osuga J, Okazaki H, Tamura Y, Iizuka Y, Shionoiri F, Ohashi K, Harada K, Gotoda T, Nagai R, Ishibashi S, Yamada N: Sterol regulatory element-binding protein-1 is regulated by glucose at the transcriptional level. *J Biol Chem* 275:31069–31077, 2000
20. Matsuzaka T, Shimano H, Yahagi N, Amemiya-Kudo M, Okazaki H, Tamura Y, Iizuka Y, Ohashi K, Tomita S, Sekiya M, Hasty A, Nakagawa Y, Sone H, Toyoshima H, Ishibashi S, Osuga J, Yamada N: Insulin-independent induction of sterol regulatory element-binding protein-1c expression in the livers of streptozotocin-treated mice. *Diabetes* 53:560–569, 2004
21. Horton JD, Bashmakov Y, Shimomura I, Shimano H: Regulation of sterol regulatory element binding proteins in livers of fasted and refed mice. *Proc Natl Acad Sci U S A* 95:5987–5992, 1998
22. Yahagi N, Shimano H, Hasty AH, Amemiya-Kudo M, Okazaki H, Tamura Y, Iizuka Y, Shionoiri F, Ohashi K, Osuga J, Harada K, Gotoda T, Nagai R, Ishibashi S, Yamada N: A crucial role of sterol regulatory element-binding protein-1 in the regulation of lipogenic gene expression by polyunsaturated fatty acids. *J Biol Chem* 274:35840–35844, 1999
23. Sekiya M, Yahagi N, Matsuzaka T, Najima Y, Nakakuki M, Nagai R, Ishibashi S, Osuga J, Yamada N, Shimano H: Polyunsaturated fatty acids ameliorate hepatic steatosis in obese mice by SREBP-1 suppression. *Hepatology* 38:1529–1539, 2003
24. Lin J, Yang R, Tarr PT, Wu PH, Handschin C, Li S, Yang W, Pei L, Uldry M, Tontonoz P, Newgard CB, Spiegelman BM: Hyperlipidemic effects of dietary saturated fats mediated through PGC-1beta coactivation of SREBP. *Cell* 120:261–273, 2005
25. Ide T, Shimano H, Yahagi N, Matsuzaka T, Nakakuki M, Yamamoto T, Nakagawa Y, Takahashi A, Suzuki H, Sone H, Toyoshima H, Fukamizu A, Yamada N: SREBPs suppress IRS-2-mediated insulin signalling in the liver. *Nat Cell Biol* 6:351–357, 2004
26. Takahashi A, Motomura K, Kato T, Yoshikawa T, Nakagawa Y, Yahagi N, Sone H, Suzuki H, Toyoshima H, Yamada N, Shimano H: Transgenic mice overexpressing nuclear SREBP-1c in pancreatic β-cells. *Diabetes* 54:492–499, 2005
27. Diraison F, Parton L, Ferre P, Foufelle F, Briscoe CP, Leclerc I, Rutter GA: Over-expression of sterol-regulatory-element-binding protein-1c (SREBP1c) in rat pancreatic islets induces lipogenesis and decreases glucose-stimulated insulin release: modulation by 5-aminoimidazole-4-carboxamide ribonucleoside (AICAR). *Biochem J* 378:769–778, 2004
28. Kakuma T, Lee Y, Higa M, Wang Z, Pan W, Shimomura I, Unger RH: Leptin, troglitazone, and the expression of sterol regulatory element binding proteins in liver and pancreatic islets. *Proc Natl Acad Sci U S A* 97:8536–8541, 2000
29. Martinez SC, Cras-Meneur C, Bernal-Mizrachi E, Permutt MA: Glucose regulates Foxo1 through insulin receptor signaling in the pancreatic islet β-cell. *Diabetes* 55:1581–1591, 2006

30. Tuttle RL, Gill NS, Pugh W, Lee JP, Koeberlein B, Furth EE, Polonsky KS, Naji A, Birnbaum MJ: Regulation of pancreatic beta-cell growth and survival by the serine/threonine protein kinase Akt1/PKBalpha. *Nat Med* 7:1133–1137, 2001
31. Bernal-Mizrachi E, Fatrai S, Johnson JD, Ohsugi M, Otani K, Han Z, Polonsky KS, Permutt MA: Defective insulin secretion and increased susceptibility to experimental diabetes are induced by reduced Akt activity in pancreatic islet beta cells. *J Clin Invest* 114:928–936, 2004
32. Fatrai S, Elghazi L, Balcazar N, Cras-Meneur C, Krits I, Kiyokawa H, Bernal-Mizrachi E: Akt induces β-cell proliferation by regulating cyclin D1, cyclin D2, and p21 levels and cyclin-dependent kinase-4 activity. *Diabetes* 55:318–325, 2006
33. Kitamura T, Nakae J, Kitamura Y, Kido Y, Biggs WH III, Wright CV, White MF, Arden KC, Accili D: The forkhead transcription factor Foxo1 links insulin signaling to Pdx1 regulation of pancreatic beta cell growth. *J Clin Invest* 110:1839–1847, 2002
34. Okamoto H, Hribal ML, Lin HV, Bennett WR, Ward A, Accili D: Role of the forkhead protein FoxO1 in beta cell compensation to insulin resistance. *J Clin Invest* 116:775–782, 2006
35. Coppola T, Frantz C, Perret-Menoud V, Gattesco S, Hirling H, Regazzi R: Pancreatic beta-cell protein granuphilin binds Rab3 and Munc-18 and controls exocytosis. *Mol Biol Cell* 13:1906–1915, 2002
36. Torii S, Zhao S, Yi Z, Takeuchi T, Izumi T: Granuphilin modulates the exocytosis of secretory granules through interaction with syntaxin 1a. *Mol Cell Biol* 22:5618–5626, 2002
37. Gomi H, Mizutani S, Kasai K, Itohara S, Izumi T: Granuphilin molecularly docks insulin granules to the fusion machinery. *J Cell Biol* 171:99–109, 2005
38. Kato T, Shimano H, Yamamoto T, Yokoo T, Endo Y, Ishikawa M, Matsuzaka T, Nakagawa Y, Kumadaki S, Yahagi N, Takahashi A, Sone H, Suzuki H, Toyoshima H, Hasty AH, Takahashi S, Gomi H, Izumi T, Yamada N: Granuphilin is activated by SREBP-1c and involved in impaired insulin secretion in diabetic mice. *Cell Metab* 4:143–154, 2006
39. Shimano H, Shimomura I, Hammer RE, Herz J, Goldstein JL, Brown MS, Horton JD: Elevated levels of SREBP-2 and cholesterol synthesis in livers of mice homozygous for a targeted disruption of the SREBP-1 gene. *J Clin Invest* 100:2115–2124, 1997
40. Scharp DW, Kemp CB, Knight MJ, Ballinger WF, Lacy PE: The use of ficoll in the preparation of viable islets of Langerhans from the rat pancreas. *Transplantation* 16:686–689, 1973
41. Schultz V, Sussman I, Bokvist K, Tornheim K: Bioluminometric assay of ADP and ATP at high ATP/ADP ratios: assay of ADP after enzymatic removal of ATP. *Anal Biochem* 215:302–304, 1993
42. Noushmehr H, D'Amico E, Farilla L, Hui H, Wawrowsky KA, Mlynarski W, Doria A, Abumrad NA, Perfetti R: Fatty acid translocase (FAT/CD36) is localized on insulin-containing granules in human pancreatic β-cells and mediates fatty acid effects on insulin secretion. *Diabetes* 54:472–481, 2005
43. Ono H, Shimano H, Katagiri H, Yahagi N, Sakoda H, Onishi Y, Anai M, Ogihara T, Fujishiro M, Viana AY, Fukushima Y, Abe M, Shojima N, Kikuchi M, Yamada N, Oka Y, Asano T: Hepatic Akt activation induces marked hypoglycemia, hepatomegaly, and hypertriglyceridemia with sterol regulatory element binding protein involvement. *Diabetes* 52:2905–2913, 2003
44. Nakagawa Y, Shimano H, Yoshikawa T, Ide T, Tamura M, Furusawa M, Yamamoto T, Inoue N, Matsuzaka T, Takahashi A, Hasty AH, Suzuki H, Sone H, Toyoshima H, Yahagi N, Yamada N: TFE3 transcriptionally activates hepatic IRS-2, participates in insulin signaling and ameliorates diabetes. *Nat Med* 12:107–113, 2006
45. Iwatsuka H, Shino A, Suzuoki Z: General survey of diabetic features of yellow KK mice. *Endocrinol Jpn* 17:23–35, 1970
46. Browning LM: n-3 Polyunsaturated fatty acids, inflammation and obesity-related disease. *Proc Nutr Soc* 62:447–453, 2003

THE JOURNAL OF BIOLOGICAL CHEMISTRY VOL. 283, NO. 30, pp. 21220–21229, July 25, 2008

Cyclin-dependent Kinase Inhibitor, p21$^{WAF1/CIP1}$, Is Involved in Adipocyte Differentiation and Hypertrophy, Linking to Obesity, and Insulin Resistance*[S]

Received for publication, March 6, 2008 Published, JBC Papers in Press, April 29, 2008, DOI 10.1074/jbc.M801824200

Noriyuki Inoue[‡], Naoya Yahagi[§], Takashi Yamamoto[‡], Mayumi Ishikawa[‡], Kazuhisa Watanabe[‡], Takashi Matsuzaka[§], Yoshimi Nakagawa[‡], Yoshinori Takeuchi[‡], Kazuto Kobayashi[‡], Akimitsu Takahashi[‡], Hiroaki Suzuki[‡], Alyssa H. Hasty[¶], Hideo Toyoshima[‡], Nobuhiro Yamada[‡], and Hitoshi Shimano[‡§1]

From the [‡]Department of Internal Medicine (Metabolism and Endocrinology) and [§]Graduate School of Comprehensive Human Sciences and Center for Tsukuba Advanced Research Alliance, University of Tsukuba, 1-1-1 Tennodai, Tsukuba, Ibaraki, 305-8575, Japan and [¶]Department of Molecular Physiology and Biophysics, Vanderbilt University, Nashville, Tennessee 37232

Both adipocyte hyperplasia and hypertrophy are determinant factors for adipocyte differentiation during the development of obesity. p21$^{WAF1/CIP1}$, a cyclin-dependent kinase inhibitor, is induced during adipocyte differentiation; however, its precise contribution to this process is unknown. Using both *in vitro* and *in vivo* systems, we show that p21 is crucial for maintaining adipocyte hypertrophy and obesity-induced insulin resistance. The absence of p21 in 3T3-L1 fibroblasts by RNA-mediated interference knockdown or in embryonic fibroblasts from p21$^{-/-}$ mice impaired adipocyte differentiation, resulting in smaller adipocytes. Despite normal adipose tissue mass on a normal diet, p21$^{-/-}$ mice fed high energy diets had reduced adipose tissue mass and adipocyte size accompanied by a marked improvement in insulin sensitivity. Knockdown of p21 in enlarged epididymal fat of diet-induced obese mice and also in fully differentiated 3T3-L1 adipocytes caused vigorous apoptosis by activating p53. Thus, p21 is involved in both adipocyte differentiation and in protecting hypertrophied adipocytes against apoptosis. Via both of these mechanisms, p21 promotes adipose tissue expansion during high fat diet feeding, leading to increased downstream pathophysiological consequences such as insulin resistance.

The process of adipocyte differentiation has been extensively characterized in cultures of preadipocyte clonal cell lines such as mouse 3T3-L1 and 3T3-F442A (1, 2). Adipogenesis requires a sequence of events including growth arrest of proliferating preadipocytes, coordinated reentry into the cell cycle with limited clonal expansion, and growth arrest before terminal differentiation during which lipid accumulation occurs. Thus, it is reasonable to assume that factors involved in cell cycle regulation may have important roles in the adipocyte differentiation process. Cell cycle progression in mammals is governed by various complexes of cyclins and cyclin-dependent kinases (CDKs)[2] as well as their inhibitors, of which p21 and p27 are the most widely studied. It was previously suggested that expression of p21 and p27 is changed during the adipogenesis (3). p21 has been reported to be induced by Foxo1 and has been implicated in entry of adipocytes into the clonal expansion phase of adipogenesis; meanwhile, p27 is critical for adipocyte hyperplasia (3–5). The expression of both p21 and p27 is altered during adipocyte differentiation; however, their precise role in adipogenesis, especially at the time of terminal differentiation, remains unclear.

Obesity is caused by over-nutrition and decreased physical activity and is characterized by excess storage of lipids in adipose tissue, which can be accounted for by both adipocyte hyperplasia and hypertrophy. Obesity often precedes insulin resistance and precipitates type 2 diabetes and cardiovascular diseases (6). Impaired adipocyte differentiation is also related to insulin resistance. Based upon the potential roles of CDK inhibitors in cell cycle progression and apoptosis, it is reasonable to speculate that CDK inhibitors could be involved in obesity and insulin resistance through regulation of adipocyte differentiation and adipose tissue growth.

p21$^{WAF1/CIP1}$ is the major CDK inhibitor and halts the cell cycle at G_1 (Refs. 7–10; for review, see Refs. 11 and 12). p21 is a well known target of p53, a stress response. In addition to causing G_1 arrest, p21 protects cells from apoptosis (12). We recently found that p21 is a direct gene target of SREBPs, crucial transcription factors involved in lipogenesis and adipogenesis (13, 14). We also reported that p21 expression was highly upregulated in hypertrophic adipose tissue and in the liver in models of obesity (15, 16). These data prompted us to explore the role of p21 in adipocyte differentiation and hypertrophy and to determine the involvement of p21 in obesity and insulin resistance.

* This research was supported in part by Grant-in-Aid for Scientific Research and Scientific Research on Priority Areas, 2006, 1805200 from the Ministry of Education, Science, Sports, and Culture. The costs of publication of this article were defrayed in part by the payment of page charges. This article must therefore be hereby marked "*advertisement*" in accordance with 18 U.S.C. Section 1734 solely to indicate this fact.

[S] The on-line version of this article (available at http://www.jbc.org) contains supplemental Figs. A1–A5 and Tables A1–A3.

[1] To whom correspondence should be addressed. Tel.: 81-29-853-3053; Fax: 81-29-863-3074, E-mail: shimano-tky@umin.ac.jp.

[2] The abbreviations used are: CDK, cyclin-dependent kinase; RNAi, RNA-mediated interference; MEF, mouse embryonic fibroblast; HFHS, high fat high sucrose; PPAR, peroxisome proliferator-activated receptor; DEXA, dual energy x-ray absorptiometry; TUNEL, terminal dUTP nick-end labeling; C/EBP, CCAAT/enhancer-binding protein.

EXPERIMENTAL PROCEDURES

Cell Culture and Adipocyte Differentiation—3T3-L1 cells (ATCC) were maintained in high glucose Dulbecco's modified Eagle's medium (Invitrogen) with 10% fetal calf serum in 5% CO_2. Cells were seeded at 2.5×10^5 cell/6-cm collagen-coated dishes (BD Biosciences) (day 4) and cultured to confluence (day 2). After 2 days, cells were replaced with differentiation induction medium A (5 μg/ml insulin, 1 μM dexamethasone, and 0.5 mM isobutylmethylxanthine) (day 0). After 48 h cells were changed to differentiation induction medium B (5 mg/ml insulin) (day 2). Medium was renewed every other day.

Preparation of Recombinant Adenovirus—cDNAs encoding the full-length fragment of mouse $p21^{Waf1/Cip1}$ were integrated into adenoviral vectors. RNAi adenovirus vectors, RNAi-LacZ (LacZi), p21 RNAi-137 (137i), and p21 RNAi-275 (275i) were constructed with BLOCK-iT™ U6 RNAi Entry Vector kit and BLOCK-iT™ Adenoviral RNAi Expression system (Invitrogen). Each adenoviral vector was propagated in 293A cells and purified by cesium chloride density centrifugation (17, 18).

Oil Red O Stain—Cells were fixed with 10% formalin in phosphate-buffered saline for 10 min at 37 °C and stained with Oil Red O for 60 min at room temperature. Cells were washed with distilled water, and the retained dye was eluted by isopropanol (19).

Mice—This project was approved by The Animal Care Committee of University of Tsukuba and performed under its guidelines. The $p21^{waf1/Cip1}$ knock-out mice (B6;129S2-*Cdkn1a*$^{tm1Tyj/J}$) were originally purchased from CLEA Japan Inc. and The Jackson Laboratory, provided by Dr. Tyler Jacks (20) and were backcrossed onto the C57BL/6J background within our colony for five or more generations. Mice were genotyped by PCR according to methods provided by The Jackson Laboratory. Mice were maintained on a normal chow diet for a 14-h light/10-h dark cycle. For diet-induced obesity, the mice were fed on a high fat high sucrose (HFHS) diet as previously described (21) at 10 weeks of age for 6 (or indicated) weeks. We performed weekly collections of blood for metabolic analysis (measurement of blood glucose, insulin, triglyceride, total cholesterol, and free fatty acid) and measured body weight. They were subjected to intravenous glucose tolerance tests 4 weeks after the HFHS diet started, insulin tolerance tests 5 weeks after the diet started, dual energy x-ray absorptiometry (DEXA) analysis, and sacrifice at 6 weeks. Tissue samples were fixed in 10% formalin for microscopy analysis and preserved in liquid N_2 for the Northern blot analysis.

DEXA Analysis—PIXImus2 DEXA (GE Medical Systems LUNAR) was used to measure lean body tissue and percent fat mass (22).

Determination of Adipocyte Number and Size—Epididymal fat pads from normal mice (~50 mg) and HFHS-fed mice (~150 mg) were fixed in osmium tetroxide-collidine buffer for 3 days. Adipocytes of diameter from 25 to 125 μm in normal mice or from 25 to 250 μm in HFHS mice were collected by filtration through 25-, 125-, and 250-μm nylon screens. Size and number of adipocytes were measured with a Z-2 Coulter counter for normal mice and a Multisizer 3 Coulter counter for HFHS mice (Beckman Coulter) as previously described (22–24).

Metabolic Studies—Glucose tolerance tests were performed on male mice fasted overnight (9–12 h). Glucose solutions were injected at 2 g/kg of body weight via tail vein. Blood glucose and insulin were measured 0, 5, 15, 30, and 60 min after injection. Insulin tolerance tests were performed on male mice fasted for 3 h. Mice were intraperitoneally injected with human regular insulin at 0.5 units/kg or 0.75 units/kg of body weight (Humulin R 40 units/ml, Eli Lilly), and blood glucose was measured 0–120 min after injection with ANTSENSE II (Horiba Ltd.). Plasma glucose, triglyceride, cholesterol, and non-esterfied fatty acids were determined with Glu ICII, TG IE, T-Cho IE, and non-esterfied fatty acid IC kits from WAKO. Plasma insulin and leptin were determined with the mouse insulin enzyme-linked immunosorbent assay (ELISA) kit (TMB) (AKRIN-011T, Shibayagi) and the mouse leptin ELISA kit (Morinaga Institute of Biological Science, Inc.), respectively.

Northern Blot Analysis—Total RNA was prepared from livers, white adipose tissue, brown adipose tissue, muscle, and cultured cells using TRIzol reagent (Invitrogen). For Northern blot analysis, equal aliquots of total RNA from 5–6 mice and culture cells were pooled (5–10 μg of total RNA), denatured with formaldehyde and formamide, subjected to electrophoresis in a 1% agarose gel, and transferred to Hybond N membranes (Amersham Biosciences) for hybridization. cDNA probes were labeled with [α-^{32}P]dCTP (3,000–10,000 cpm) using Rediprime™ Random Prime Labeling System (Amersham Biosciences). The filters were hybridized with the radiolabeled probe in Rapid-hyb buffer (Amersham Biosciences) at 65 °C and washed in 0.1 × SSC, 0.1% SDS at 65 °C. Blots were exposed to Kodak BIOMAX MS1 (Eastman Kodak Co.) and BAS 2500 with BAStation software (Fuji Photo Film).

Cell Proliferation Assay—For determination of cell proliferation, a 5-bromo-2′-deoxyuridine labeling and detection kit I was used according to the manufacturer's instructions (Roche Applied Science).

Apoptosis Assay—For the assessment of apoptosis, the In Situ Cell Death Detection kit (Roche Applied Science) was used. The test principle of this kit was labeling DNA strand breaks by terminal deoxynucleotidyltransferase, which catalyzes the polymerization of labeled nucleotides to free 3′-OH DNA ends in a template-independent manner (TUNEL reaction).

Immunoblot Analysis—Cells were harvested in 1% Triton X-100 buffer (25 mM Hepes (pH 7.9), 50 mM KCl, 5 mM EDTA, 5 mM $MgCl_2$, 1% Triton X-100, 1 mM dithiothreitol, and protease inhibitor (Roche Applied Science)). Protein concentrations were determined using the BCA protein assay kit (Pierce). Samples were fractionated on 8, 12, or 15% SDS-PAGE followed by transfer to Immobilon Transfer membranes (Millipore). Blots were subsequently incubated in Tris-buffered saline-Tween overnight at 4 °C with 1:2000 anti-$p21^{waf1}$, anti-$p27^{Kip1}$, anti-C/EBPα, anti-C/EBPβ, anti-p53 (Santa Cruz) Ser-15 phosphorylation of p53, Ser-20 phosphorylation of p53, Ser-46 phosphorylation of p53 (Cell Signaling), and α-tubulin (Calbiochem). After incubation with horseradish peroxidase-conjugated secondary antibod-

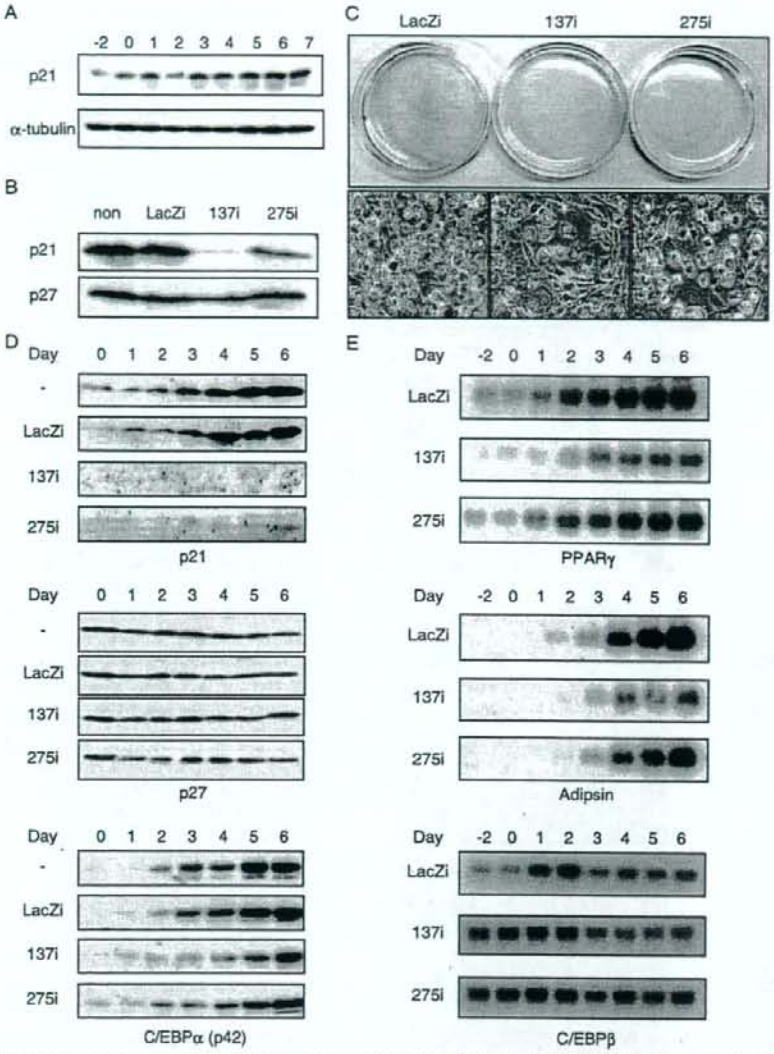

FIGURE 1. **Inhibition of adipocyte differentiation in 3T3-L1 cells by knockdown of p21.** *A*, changes of p21 protein in differentiating 3T3-L1 cells. Total cellular proteins were extracted from cells at the indicated days of differentiation and subjected to immunoblot analysis with antibodies against p21 and α-tubulin as a loading control. *B*, efficacy of p21 knockdown in 3T3-L1 preadipocytes infected with p21RNAi adenoviruses. Expression of p21 and p27 level is shown by immunoblotting 24 h after the infection of p21 RNAi adenovirus (*137i* or *275i*) or LacZi adenovirus (*LacZi*) as a negative control. Note that 137i exhibits nearly complete suppression with a higher efficiency of p21 knockdown than 275i. *C*, effect of p21 gene knockdown on adipocytes differentiation. 3T3-L1 adipocytes were infected with adenoviruses at day 3. The Oil Red O staining of cells from day 6 post-differentiation induction is shown. *D* and *E*, time course analysis of protein (*D*) and mRNA (*E*) expression in 3T3-L1 cells after infection of p21 RNAi adenoviruses at day 3. Cellular total RNA (5 μg) and protein (80 μg) were subjected to SDS-PAGE followed by immunoblot analysis for p21, p27, and C/EBPα (*D*) and to Northern blot analysis for PPARγ, adipsin, and C/EBPβ (*E*), respectively.

ies, blots were detected by ECL or ECL Advance Western blotting detection kit (Amersham Biosciences).

In Vivo Adenovirus Injection into White Adipose Tissue—After 3 weeks of HFHS feeding, mice were anesthetized by halothane before tissue dissection. The adenovirus (2.5×10^{11} optical particle unit) was injected on each side of the epididymal fat pad (25).

Statistical Analysis—Data are expressed as the mean ± S.E. Statistical significance was assessed using the Student's *t* test. Data sets involving more than two groups are assessed by Dunnett's test (SAS Institute Inc.).

RESULTS

Effects of the Acute Absence of p21 on Adipocyte Differentiation in Vitro—3T3-L1 fibroblasts were differentiated into adipocytes, and p21 expression was assessed. Consistent with previous works, there was a rapid induction of p21 protein at the time of differentiation into adipocytes (Fig. 1*A*) (3). Expression of p21 was sustained at both the mRNA and protein levels during terminal differentiation and during the subsequent hypertrophic phase of lipid accumulation. To determine the effects of acute p21 deficiency, knockdown of p21 using two different adenoviral vectors with RNAi (137i and 275i) before induction of differentiation was performed (Fig. 1*B*). p21 deficiency caused a dose-dependent suppression of adipocyte differentiation as assessed by Oil Red O staining (Fig. 1*C*). The inhibition of p21 resulted in no changes in p27 levels (Fig. 1*D*). However, reduction in p21 levels was accompanied by reduced levels of C/EBPα and PPARγ, transcription factors involved in adipocyte differentiation, along with adipsin, a marker for adipogenesis (Fig. 1*E*). However, C/EBPβ, known to function at an initial stage of adipogenesis was rather enhanced by p21 inhibition, suggesting that the absence of p21 might impair the later stage of adipocyte differentiation (Fig. 1*E*).

Effects of the Chronic Absence of p21 during Adipocyte Differentiation in Vitro—To determine the effect of chronic absence of p21, mouse embryonic fibroblasts (MEFs) from $p21^{-/-}$ mice were induced to differentiate into adipocytes (supplemental Fig. A1). Before differentiation, $p21^{-/-}$ MEF cells exhibited an increased cell number and uptake of 5-bromo-2′-deoxyuridine as compared with $p21^{+/+}$ control cells, indicating enhanced cell